



1 **Reviews and syntheses: Methane biogeochemistry in Sundarbans mangrove ecosystem, NE coast**  
2 **of India; a box modeling approach**

3 **Manab Kumar Dutta<sup>1\*</sup>, Sandip Kumar Mukhopadhyay<sup>2</sup>**

4 <sup>1</sup>Geoscience Division, Physical Research Laboratory, Ahmedabad – 380009, India

5 <sup>2</sup>Department of Marine Science, University of Calcutta. 35, Ballygunge Circular Road, Kolkata -  
6 700019, West Bengal, India

7 **\*Author for correspondence:** Postdoctoral Fellow. Geoscience Division, Physical Research  
8 Laboratory, Ahmedabad – 380009, India. Email: [manabdutta.1987@gmail.com](mailto:manabdutta.1987@gmail.com)

9 **Abstract:**

10 Biogeochemical cycling of CH<sub>4</sub> was studied in Sundarbans mangrove system during June 2010 to  
11 December 2012. The sediment was CH<sub>4</sub> supersaturated with mean production potential of 3547 &  
12 48.88 μmol m<sup>-3</sup> d<sup>-1</sup>, respectively in case of intertidal (0 – 25 cm depth) & sub-tidal sediments (first 5  
13 cm depth). This induces significant CH<sub>4</sub> out-flux from sediment to estuary via advective and diffusive  
14 transports. Mean advective (from intertidal sediment) and diffusive (from sub-tidal sediment) CH<sub>4</sub>  
15 fluxes were 159.52 μmol m<sup>-2</sup> d<sup>-1</sup> and 8.45 μmol m<sup>-2</sup> d<sup>-1</sup>, respectively. Intertidal sediment CH<sub>4</sub> emission  
16 rate was about 4 times higher than surface layer CH<sub>4</sub> oxidation rate; indicating petite methanotrophic  
17 activity in mangrove sediment. Mean CH<sub>4</sub> concentration in estuarine surface and bottom waters were



18 69.90 and 56.17nM, respectively. CH<sub>4</sub> oxidation in estuarine water column being 14 times higher than  
19 water - atmosphere exchange is considered as principal CH<sub>4</sub> removal mechanism in this estuary. Mean  
20 CH<sub>4</sub> mixing ratio over the mangrove forest atmosphere was 2.013ppmv. The ecosystem acts a source  
21 of CH<sub>4</sub> to the upper atmosphere having mean biosphere - atmosphere exchange flux of 0.086 mg m<sup>-2</sup>  
22 d<sup>-1</sup>. Mean CH<sub>4</sub> photo-oxidation rate in the mangrove forest atmosphere was 3.25 x 10<sup>-9</sup> mg cm<sup>-3</sup> d<sup>-1</sup>  
23 and is considered as principal CH<sub>4</sub> removal mechanism in the forest atmosphere. Finally, a box model  
24 presenting CH<sub>4</sub> biogeochemistry in Sundarbans biosphere reserve has been drafted and was used to  
25 demonstrate CH<sub>4</sub> budget in this ecosystem.

26 Keywords: methane, biogeochemistry, budget, mangrove, Sundarbans, India.

## 27 **1. Introduction:**

28 Methane (CH<sub>4</sub>) is the key gaseous constituent of global carbon biogeochemical cycle in anaerobic  
29 environment. In carbon biogeochemical cycle, quantitatively 1% of the CO<sub>2</sub> fixed annually by  
30 photosynthesis is converted back to CO<sub>2</sub> by microorganisms via CH<sub>4</sub>; the amount of CH<sub>4</sub> annually  
31 cycled in this way is around 1 billion tones (Rudolf et al. 2006). The atmospheric CH<sub>4</sub> mixing ratio  
32 increased from 0.72 ppbv in 1750 to 1.77 ppbv in 2005 (IPCC, 2007); creating a potential threat  
33 towards earth's climate as CH<sub>4</sub> global warming potential is 26 times higher than CO<sub>2</sub> (Lelieveld et al.  
34 1993). The cause of this large augmentation is not fully understood, but it is probably related to a surge



35 in CH<sub>4</sub> emission from wetlands that contributes approximately 20 - 39% of the annual global CH<sub>4</sub>  
36 budget (Hoehler et al. 2014).

37 Presenting accurate wetland CH<sub>4</sub> budget is very important for projecting the future climate. But, the  
38 primary problems in attempting to develop accurate CH<sub>4</sub> budget is the large spatial and temporal (Ding  
39 et al. 2003) variability in CH<sub>4</sub> emissions that reported all over the world. Being an integrated part of  
40 coastal wetlands, mangroves are relatively very less studied ecosystem with respect to CH<sub>4</sub>  
41 biogeochemistry (Barnes et al. 2006; Biswas et al. 2007; Bouillon et al. 2007c; Kristensen et al. 2008).  
42 Consequently, presenting wider CH<sub>4</sub> and carbon budgets for mangrove ecosystem globally is  
43 problematic.

44 Mangroves are one of the most productive coastal ecosystems and are characterized by high turnover  
45 rates of organic matter, both in the water column and in sediment. The organic matter mineralization in  
46 sediment is a multi-step process, which begins with an enzymatic hydrolysis of polymeric material to  
47 soluble monomeric and oligomeric compounds. Under oxic conditions the organic carbon (OC) is  
48 directly mineralized to carbon dioxide and water. But, the mangrove sediments are rich in clay content  
49 that reduces the porosity of the sediment and helps in the formation and retention of anoxic condition  
50 (Dutta et al. 2013). OC mineralization in anaerobic environment is typically complex involving various  
51 microbes in initial de-polymerization followed by fermentative microbial break down of complex  
52 organic compounds to small moieties. The end products of the fermentation process used by  
53 methanogens in the final step of anaerobic decomposition can also be used by microbial groups that



54 utilize a variety of inorganic terminal electron acceptors (TEAs) in their metabolism (Megonigal et al.  
55 2004). The competitiveness, and thus relative importance, of these TEAs is thought to be controlled  
56 primarily by their thermodynamic favourability in the following order:  $\text{NO}_3^-$  (denitrification), Fe (III)  
57 (iron reduction), Mn (III, IV) (manganese reduction), and  $\text{SO}_4^{2-}$  (sulphate reduction) (Keller et al., 2013).  
58 Methanogenesis remains suppressed by more favourable TEA-reducing processes and begins when all  
59 those TEAs have been consumed and electron donors are in surplus. In fact  $\text{CH}_4$  is produced by  
60 fermentative disproportionation reaction of low molecular compounds (e.g. acetate) or reduction of  $\text{CO}_2$   
61 by hydrogen or simple alcohols (Canfield et al. 2005) depending upon redox condition of sediment,  
62 which is reported to be  $\leq 150$  mV for the process of methanogenesis (Wang et al. 1993). The  
63 sedimentary produced  $\text{CH}_4$  partially escapes through diffusion and direct ebullition to the atmosphere  
64 after partially being oxidized at surface (aerobic oxidation) and subsurface sediments (anaerobic  
65 oxidation), while the remaining dissolves in pore water resulting super-saturation. During low tide  
66 condition, the  $\text{CH}_4$  rich pore water transports to the adjacent creeks and estuaries depending upon  
67 hypsometric gradient. In addition,  $\text{CH}_4$  produced in the underlying sediment of the estuary (sub-tidal  
68 sediment) diffuses upward to further enrich the dissolved  $\text{CH}_4$  level in estuarine water column.

69 In the estuarine water column, the supplied  $\text{CH}_4$  is partly oxidized to  $\text{CO}_2$  by methanotrophs, which use  
70  $\text{CH}_4$  as the sole carbon source (Hanson and Hanson, 1996). Aerobic  $\text{CH}_4$  oxidation in the aquatic  
71 systems significantly reduces the  $\text{CH}_4$  flux across water – atmosphere interface. In case of stratified  
72 systems like lakes, pelagic  $\text{CH}_4$  oxidation can consume up to 90 % of the dissolved  $\text{CH}_4$  (Utsumi et al.



73 1998a; Kankaala et al. 2006), whereas in the well-mixed estuaries, CH<sub>4</sub> oxidation is believed to be  
74 much less efficient (Abril et al. 2007). The CH<sub>4</sub> that escapes from microbial oxidation partially emits  
75 from estuary across water - atmosphere interface and remaining exports to adjacent continental shelves  
76 region.

77 The emitted CH<sub>4</sub> from sediment – atmosphere and water – atmosphere interfaces of the mangrove  
78 ecosystem enrich the atmospheric CH<sub>4</sub> mixing ratio at a regional level (Mukhopadhyay et al. 2002) and  
79 further participates in complex atmospheric CH<sub>4</sub> cycle. In the mangrove forest environment, emitted  
80 CH<sub>4</sub> partially exchanges across biosphere - atmosphere interface depending upon micrometeorological  
81 conditions; while the major fraction undergoes photo-oxidation depending upon ambient NO<sub>x</sub> level. A  
82 schematic diagram of atmospheric CH<sub>4</sub> photo-oxidation with/without NO<sub>x</sub> concentration is presented in  
83 Fig.1 (modified from Wayne, 1991).

84 This study aimed to report production, oxidation, distribution and fluxes of CH<sub>4</sub> in different sub-  
85 ecosystems of Sundarbans for complete understanding of CH<sub>4</sub> biogeochemistry in the estuarine  
86 mangrove environment. Beyond this primary objective, another main objective of this study was to  
87 demonstrate a comprehensive CH<sub>4</sub> budget for Sundarbans biosphere reserve.

## 88 **2. Study location:**

89 Sundarbans is the largest single block of tidal mangrove forest in the world, situated over India and  
90 Bangladesh at the land ocean boundary of Ganges-Brahmaputra delta and the Bay of Bengal. This



91 extensive natural mangrove forest was inscribed as a UNESCO world heritage site and covers an area of  
92 10,200 sq. km of which 4200 sq. km of reserved forest is spread over India and rest part is in  
93 Bangladesh. The Indian Sundarbans Biosphere Reserve (SBR) is extended over an area of 9600 km<sup>2</sup>  
94 constituted of 1800 sq km estuarine waterways and 3600 sq. km reclaimed areas along with above  
95 stated mangrove reserve forest. The forest is about 140 km in length from east to west and extends  
96 approximately 50 – 70 km from the southern margin of the Bay of Bengal towards the north. The Indian  
97 part of the Sundarbans mangrove delta is crisscrossed by the estuarine phases of several rivers namely  
98 Mooriganga, Saptamukhi, Thakuran, Matla, Bidya, Gosaba and Haribhanga forming a sprawling  
99 archipelago of 102 islands out of which 54 are reclaimed for human settlement and rest are virgin. One  
100 of these virgin Islands is the Lothian Island, which is situated at the buffer zone of the Sundarbans  
101 Biosphere Reserve covering an area of 38 km<sup>2</sup>. This island completely intertidal and occupied by thick,  
102 robust and resilient mangroves trees with a mean height of < 10 m. Among the mangroves, *Avicennia*  
103 *alba*, *Avicennia marina* and *Avicennia officinalis* are the dominant species, *Excoecaria agallocha* and  
104 *Heritiera fomes* are thinly distributed and *Ceriops decandra* is found scattered all over the island. The  
105 mangrove sediment is silty clay in nature and composed of quartzo-feldspathic minerals like quartz,  
106 albite and microline. The adjacent estuarine system of the island is Saptamukhi which has no perennial  
107 source of freshwater and receives significant amounts of agricultural and anthropogenic runoff  
108 especially during monsoon. Climate in the study area is characterized by premonsoon (February –  
109 May), south west monsoon (June – September) and north east monsoon or postmonsoon (October –



110 January). Based on the above the Lothian Island and associated Saptamukhi estuary have been chosen  
111 for studying CH<sub>4</sub> biogeochemical cycle in the Sundarbans mangrove environment. A location map of  
112 Sundarbans showing Lothian Island and Saptamukhi estuary in the subset is presented in Fig.2.

### 113 **3. Materials and methods:**

114 The present study was carried out during June 2010 to December 2012 to cover the seasonal variation in  
115 the study area. Sediment and atmospheric samples were collected from the intertidal mangrove  
116 sediment & watch tower located in the center of the Lothian Island (21° 42.58'N: 88°18'E),  
117 respectively. Moreover, water samples were collected from the estuarine mixing zones of the  
118 Saptamukhi estuary. The details of study design, analyzed parameters and flux calculations are  
119 described in the following sections.

120 Intertidal sediment samples were collected at different locations of the mangrove forest covering upper,  
121 mid and lower littoral zones with the help of stainless steel corers (diameter: 10 cm) with an mean  
122 penetration depth of 25 cm. Sediment cores were sectioned at 5 cm interval and collected in zipper bags  
123 for transporting to the laboratory. Surface sediment temperature was measured in-situ using  
124 thermometer. Simultaneously estuarine bottom sediment (sub-tidal) was also collected using grab  
125 samplers. CH<sub>4</sub> production was measured by anaerobic incubations of sediment samples. A small portion  
126 of sample (about 10 g) were weighed and taken in an incubation bottle (1.2 cm i.d. and 10 cm long)  
127 fitted with rubber septum. Then the bottles were flushed with pure N<sub>2</sub> for 1 min to create a completely



128 anaerobic condition. The incubation was carried out in duplicate at ambient temperature for 24 hrs. At  
129 the end of incubation 1 ml gas sample was withdrawn from the headspace through the rubber stopper  
130 using a gas-tight glass syringe (Lu et al. 1999). CH<sub>4</sub> accumulation in the headspace was determined by  
131 gas chromatography (Varian CP3800 GC) fitted with chrompack capillary column (12.5 m x 0.53 mm)  
132 and a flame ionization detector (FID) having a mean relative uncertainty of ± 2.9 % with reference to  
133 the purity of nitrogen for CH<sub>4</sub> as blank. CH<sub>4</sub> production was calculated according to CH<sub>4</sub> accumulation  
134 in the headspace, the headspace volume and volume of samples.

135 Wet sediment samples (both intertidal and sub-tidal) are processed for measurement of CH<sub>4</sub>  
136 concentration according to Knab et al. 2009 followed by measurement of headspace for CH<sub>4</sub> by gas  
137 chromatography as described above. The nitrate, nitrite and ammonia concentrations of the sediment  
138 samples were measured taking 2M KCl extract of sediment followed by standard spectrophotometric  
139 method (Grasshoff 1983). CH<sub>4</sub> oxidation was measured for intertidal surface sediment only, following  
140 incubation with CH<sub>4</sub> spiked air. A fixed volume of surface sediment (~6 ml) was taken in 60 ml flasks  
141 fitted with rubber septum and head space air (21% O<sub>2</sub>) was spiked with 100 μL CH<sub>4</sub> L<sup>-1</sup> (10 ppmv CH<sub>4</sub>,  
142 procured from Chemtron Science Laboratories Pvt. Ltd.). These flasks were incubated in duplicate at  
143 ambient temperature for 4 days. Gas samples from the head-space was drawn immediately at the onset  
144 of incubation and at 24 hours interval till the end for analyzing CH<sub>4</sub> concentration using gas  
145 chromatograph as described earlier. CH<sub>4</sub> oxidation was calculated according to decrease of CH<sub>4</sub>  
146 concentration in the headspace, the headspace volume and volume of sediment samples.





147 During low tide condition  $\text{CH}_4$  emission from the intertidal sediment surface to the atmosphere was  
148 measured using static Perspex chamber method (Purvaja et al. 2004). The chambers were placed in the  
149 sediment for a particular duration and  $\text{CH}_4$  emission rate was calculated based on the enrichment of  $\text{CH}_4$   
150 mixing ratio inside the chamber in comparison to the ambient air. Mixing ratio of  $\text{CH}_4$  was measured by  
151 gas chromatography as described earlier. Advective  $\text{CH}_4$  fluxes from intertidal forest sediment to the  
152 estuarine water column ( $F_{\text{ISW}}$ ) were computed as (Reay et al. 1995):  $F_{\text{ISW}} = \Phi \times v \times C$ ; where,  $\Phi =$   
153 porosity of sediment = 0.58 (Dutta et al. 2013),  $v =$  mean linear velocity =  $d\Phi^{-1}$  ( $d =$  specific discharge),  
154  $C =$  pore water  $\text{CH}_4$  concentration in intertidal sediment. The specific discharge for the intertidal  
155 sediment was recorded by measuring the rate of accumulation of pore water in an excavated pit of  
156 known surface area (Dutta et al. 2015b). This was done during low tide condition in the intertidal flat at  
157 100 m intervals along with receding water level. Diffusive  $\text{CH}_4$  flux from sub-tidal sediment to estuary  
158 was calculated using Fick's law of diffusion (Sansone et al. 2004).

159 Collection and analysis of dissolved  $\text{CH}_4$  concentration using gas chromatograph for estuarine water has  
160 been described elsewhere (Dutta et al. 2013). For measurement of  $\text{CH}_4$  oxidation water was filled in pre-  
161 cleaned (acid washed and sterilized) septum fitted incubation bottles (in a batch of 12 bottles) from  
162 Niskin samplers with gentle overflowing and sealed with no air bubbles. Immediately after collection  
163 two bottles are poisoned with  $\text{HgCl}_2$  to stop microbial  $\text{CH}_4$  oxidation and they are considered as control  
164 for the experiment. Rest of the bottles are kept for incubation in ambient condition with two bottles  
165 withdrawn from incubation daily and were poisoned with saturated  $\text{HgCl}_2$  solution to continue the



166 incubation experiment up to a times series of 5 days. The concentrations of dissolved CH<sub>4</sub> in all  
167 incubated samples was measured to record a time series kinetics of CH<sub>4</sub> oxidation. From the time series  
168 plot, the specific rate of CH<sub>4</sub> oxidation was calculated by linear regression of the natural log of CH<sub>4</sub>  
169 concentration against time. The value of specific rate of CH<sub>4</sub> oxidation is equivalent to the slope of the  
170 regression line. Actual rates of CH<sub>4</sub> oxidation (CH<sub>4</sub> consumption rate) were calculated by the product of  
171 dissolved CH<sub>4</sub> concentration and specific rate of CH<sub>4</sub> oxidation (Utsumi et al. 1998b).

172 CH<sub>4</sub> flux across the air - water interface was calculated according to the expression (Liss and Merlivat  
173 1986):  $F_{WA} = k \Delta C$ ; where,  $\Delta C$  is the difference in concentrations ( $[CH_4]_{\text{observed}} - [CH_4]_{\text{equilibrium}}$ ) and  $k$  is  
174 the gas transfer velocity in  $\text{cm hr}^{-1}$  was calculated from wind velocity and schmidt number (Liss and  
175 Merlivat 1986). A positive value denotes flux from water to the atmosphere and vice versa. Water  
176 temperature and pH were recorded in situ using a thermometer and a portable pH meter (Orion Star  
177 A211) with a Ross combination electrode calibrated on the NBS (US National Bureau of Standards)  
178 scale (Frankignoulle and Borges 2001). Reproducibility was  $\pm 0.005$  pH units. Transparency of the  
179 water column was measured with a 15 cm diameter Secchi disc. Salinity and dissolved oxygen  
180 concentrations in surface and bottom waters were measured onboard, following the Mohr-Knudsen and  
181 Winkler titration methods, respectively (Grasshoff et al. 1983). For estimating of nitrite, nitrate and  
182 ammonia concentrations samples were collected in 1L HDPE bottles and stored on ice during  
183 transportation to the laboratory. In the laboratory concentrations were measured using standard  
184 spectrophotometric method (Grasshoff et al. 1983) and the values were added to compute dissolved



185 inorganic nitrogen concentration (DIN). For estimating of chlorophyll concentrations samples were  
186 collected in 1L amber colored bottles and stored on ice during transportation to the laboratory. In the  
187 laboratory chlorophyll concentration was measured using a standard spectrophotometric method  
188 (Parsons et al. 1992). Primary productivity and community respiration in the estuarine surface water  
189 were measured in situ by a light and dark bottle oxygen method (Parsons et al. 1992) with a relative  
190 uncertainty of  $\pm 2.5\%$ .

191 Samples for measurement of  $\text{CH}_4$  mixing ratio were collected in air sampling bulbs from both 10 m and  
192 20 m heights and transported to laboratory for analysis. Samples were analyzed using gas  
193 chromatography (Varian CP 3800GC) fitted with chrompack capillary column (12.5 m x 0.53 mm) and  
194 a flame ionization detector (FID). Two reference gas standards (10.9 ppmv and 5 ppmv, supplied by  
195 Chemtron Science Laboratories Pvt. Ltd) were used before and after every measurement. Duplicate  
196 samples were analyzed periodically and the replicate measurements were found to be within 2 - 3.2 %.  
197 Meteorological parameters like air temperature and wind velocity were simultaneously recorded at 10  
198 and 20 m heights using a portable weather monitor (Model: Davis 7440) and the value was used to  
199 calculated micrometeorological indices like friction velocity ( $U^*$ ), roughness height ( $Z_0$ ), drag  
200 coefficient and planetary boundary layer height (Ganguly et al. 2008). Biosphere - atmosphere  $\text{CH}_4$   
201 exchange flux ( $F_{\text{BA}}$ ) was calculated using the following relation (Barrett 1998; Ganguly et al. 2008):

202 
$$F_{\text{BA}} = V_C \Delta\chi.$$



203 Where,  $\Delta\chi$  = difference of mixing ratio of  $\text{CH}_4$  between 10 and 20 m height.  $V_C$  = exchange velocity  
204 which is defined as  $1 / (r_a + r_s)$  ( $r_a$  = aerodynamic resistance and  $r_s$  = surface layer resistance). Negative  
205 flux indicates net transfer from the atmosphere to the biosphere and positive flux indicates emission.  
206  $\text{CH}_4$  photo-oxidation rate (P) in the lower mangrove forest atmosphere was calculated based on the  
207 reaction ( $\text{CH}_4 + \text{OH} \rightarrow \text{CH}_3 + \text{H}_2\text{O}$ ) as:  $P = k [\text{CH}_4] [\text{OH}]$ ; where,  $k$  = rate constant of the reaction  
208 between  $\text{CH}_4$  and  $\text{OH} = 1.59 \times 10^{-20} T^{2.84} \exp(-978 / T) \text{ cm}^3 \text{ molecule}^{-1} \text{ s}^{-1}$  (Vaghjiani and Ravishankara  
209 1991).  $[\text{CH}_4]$  = mean of all  $\text{CH}_4$  mixing ratio measurements during the day time at 10 m height in the  
210 diurnal cycle and  $[\text{OH}]$  = mean of all  $\text{OH}$  radical concentrations during the day time at 10 m height in  
211 the diurnal cycle in molecules  $\text{cm}^{-3}$ .  $\text{OH}$  radical concentration was computed using photolysis frequency  
212 of  $\text{O}_3$  based on the empirical relation proposed by Ehhalt and Rohrer, 2000.

## 213 **4. Results and discussion:**

### 214 **4.1 $\text{CH}_4$ cycling in the mangrove sediment:**

215 Mean  $\text{CH}_4$  production potential of 20 - 25 cm deep sediment layer of the mangrove forest was 5831  
216  $\mu\text{mol m}^{-3} \text{ d}^{-1}$  which is about 7.9 times higher than production potential measured for 5 – 10 cm depth  
217 (table 1). Surface layer (0 – 5 cm)  $\text{CH}_4$  production potential was not measured at the study point,  
218 considering diminutive methanogenic and immense methanotrophic activity in that layer. The profile  
219 could not cover up to the end of the methanogenic sediment layer, but the value clearly indicates  
220 enormous  $\text{CH}_4$  production potential of the mangrove system with a mean of  $3547 \mu\text{mol m}^{-3} \text{ d}^{-1}$ . The



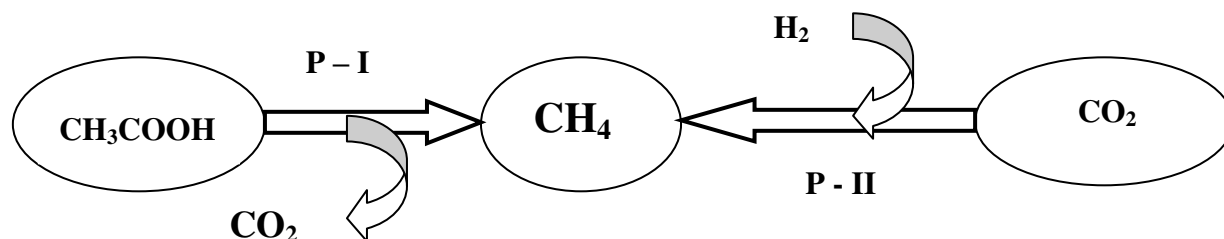
221 production potentials measured for this tropical mangrove forest sediment were within the range of that  
222 reported for pristine mangrove forest at Balandra, Mexico (Strangmann et al. 2008). On seasonal basis,  
223 highest production potential ( $4616 \pm 2666 \mu\text{mol m}^{-3} \text{d}^{-1}$ ) was noticed during postmonsoon and lowest  
224 ( $2378 \pm 1799 \mu\text{mol m}^{-3} \text{d}^{-1}$ ) during premonsoon periods. The peak postmonsoon  $\text{CH}_4$  production  
225 potential may be attributed to maximum mangrove litter fall ( $58.79 \text{ gm dry wt C m}^{-2} \text{ month}^{-1}$ ; Ray et al.  
226 2011) mediated supply of organic matter in the inter-tidal sediment and subsequently inducing higher  
227  $\text{CH}_4$  production. In contrast, high premonsoon salinity regime of the ecosystem may partially inhibited  
228  $\text{CH}_4$  production potential of the system by supplying higher  $\text{SO}_4^{2-}$  and subsequent enhanced  $\text{SO}_4^{2-}$   
229 reduction during this phase (Dutta et al. 2015b). Geochemistry of the mangrove sediment related to this  
230 study is briefly discussed elsewhere (Dutta et al. 2013) but a general trend is presented in Fig.3. The  
231 Fig.3A indicates in this inter-tidal mangrove sediment requisite redox condition for the process of  
232 methanogenesis ( $<150 \text{ mV}$ ; Wang et al. 1993) is attained at  $\approx 10 - 25 \text{ cm}$  depth while the process of  
233  $\text{SO}_4^{2-}$  reduction was prominent in the upper 20 cm sediment (Fig.3B). The decreasing trend of %OC  
234 across deep mangrove sediment indicates significant OC mineralization by anaerobic microbial  
235 metabolism (Fig.3C).

236  $\text{CH}_4$  production potential of first 5 cm deep sub-tidal sediment layer varied between  $18.72 - 85.74 \mu\text{mol}$   
237  $\text{m}^{-3} \text{d}^{-1}$  having maximal ( $77.06 \pm 12.27 \mu\text{mol m}^{-3} \text{d}^{-1}$ ) postmonsoon and minimal ( $21.28 \pm 3.63 \mu\text{mol m}^{-3}$   
238  $\text{d}^{-1}$ ) premonsoon. Mean methanogenesis rate of sub-tidal sediment (0 – 5 cm) was  $48.88 \pm 26.04 \mu\text{mol}$   
239  $\text{m}^{-3} \text{d}^{-1}$ . %OC of sub-tidal sediment surface ranged from  $1.56 \pm 0.72$  to  $2.21 \pm 0.69$  having maximum



240 concentration during postmonsoon and minimum during premonsoon period. About 35.25 % higher OC  
241 supply in sub-tidal surface layer during postmonsoon period compare to premonsoon might have caused  
242 strong redox condition favoring a higher rate of  $\text{CH}_4$  production.

243 The %OC underwent anaerobic transformation in the 5 - 10, 10 - 15, 15 - 20 and 20 - 25 cm depths  
244 were 12.7%, 9.94%, 7.64% and 8.23%, respectively. Methanogens utilize a limited number of substrates  
245 and the major pathways are through fermentation of acetate (acetoclastic) and reduction of  $\text{CO}_2$  with  $\text{H}_2$   
246 (hydrogenotrophic). The pathways for both types of methanogenesis are as follows:



249 **P - I = Acetoclastic methanogenesis; P - II = Hydrogenotrophic methanogenesis**

250 Among these two, in high  $\text{CO}_2$  rich environment acetoclastic methanogenesis is predominant over  
251 hydrogenotrophic one and approximately 70% of biologically produced  $\text{CH}_4$  originates from conversion  
252 of the methyl group of acetate to  $\text{CH}_4$  (Mayumi et al. 2013). Based on the above fact in the intertidal  
253 mangrove sediment up to the depth of penetration 25 cm, acetoclastic methanogenesis mediated OC  
254 utilization rate was  $59.58 \text{ mg m}^{-3} \text{ d}^{-1}$  resulting  $2483 \text{ } \mu\text{mol m}^{-3} \text{ d}^{-1}$  of  $\text{CH}_4$ . The estuarine bottom sediment  
255 was also OC as well as  $\text{CO}_2$  rich and  $0.82 \text{ mg m}^{-3} \text{ d}^{-1}$  of OC transformed through acetoclastic  
256 methanogenesis producing  $34.22 \text{ } \mu\text{mol m}^{-3} \text{ d}^{-1}$  of  $\text{CH}_4$ . Extrapolating the values for entire Sundarbans, it



257 is estimated that in the Sundarbans mangrove sediment (both inter and sub tidal sediments) about 22.86  
258  $\text{Ggyr}^{-1}$  of OC was transformed through methanogenic pathway resulting 15.25  $\text{Ggyr}^{-1}$  of  $\text{CH}_4$ . The  
259 mechanism also produces another radiatively active trace gas ( $\text{CO}_2$ ) as a by-product of  $\text{CH}_4$  production  
260 & acetoclastic methanogenesis mediated  $\text{CO}_2$  production rate of this mangrove forest sediment was  
261  $109.23 \text{ mg m}^{-3} \text{ d}^{-1}$ .

262 A major part of sedimentary produced  $\text{CH}_4$  dissolves in the pore water at in situ high pressure resulting  
263 significant super saturation (Dutta et al. 2013). Pore water  $\text{CH}_4$  concentrations along intertidal forest  
264 sediment depth profile are presented in table 1 indicating almost constant concentration up to 10 - 15 cm  
265 sediment layer which abruptly increase 1.79 times at 15 - 20 cm depth and further increase to 2.26 –  
266 2.76 times at 20 - 25 cm depth. On annual basis intertidal sediment pore water  $\text{CH}_4$  concentrations  
267 ranged between  $3204 \pm 1325$  to  $3639 \pm 1949$  nM, being maximal postmonsoon and minimal  
268 premonsoon periods (Dutta et al., 2015b).

269 Statistical analysis (using MINITAB version 17) was performed between pore water  $\text{CH}_4$  concentration  
270 ( $[\text{CH}_4]_{\text{PW}}$ ) vs.  $E_h$ ,  $\text{NO}_2^-$ ,  $\text{SO}_4^{2-}$ , AVS and organic carbon percentage (%OC) in order to point out key  
271 controlling factor for variability of pore water  $\text{CH}_4$  concentration in intertidal sediment. Here the  
272 dependent variable is  $[\text{CH}_4]_{\text{PW}}$  and independent variables are  $E_h$ ,  $\text{NO}_2^-$ ,  $\text{SO}_4^{2-}$ , AVS and % OC. The  
273 regression equation between dependent and independent variables are as follows:  $[\text{CH}_4]_{\text{PW}} = 10.6 -$   
274  $0.0184 E_h - 0.123 \text{NO}_2^- - 0.0076 \text{SO}_4^{2-} - 0.0693 \text{AVS} - 4.09 \% \text{OC}$  ( $R^2 = 86.6\%$ ,  $F = 7.79$ ,  $p = 0.004$ ,  $n =$



275 30). From the statistical analysis (table 2) it was found that  $[\text{CH}_4]_{\text{PW}}$  was significantly correlated with  
276 %OC ( $p = 0.004$ ) and  $E_h$  ( $p = 0.013$ ) of sediment, indicating cumulative influence of %OC and  $E_h$  on  
277 variability of  $[\text{CH}_4]_{\text{PW}}$  in this tropical mangrove forest.

278 Following same seasonal trend annual mean pore water  $\text{CH}_4$  concentrations in estuarine bottom lying  
279 sediment varied between  $2770 \pm 1039$  to  $3980 \pm 1227$  nM (Dutta et al., 2015b). Compare to the adjacent  
280 estuarine water (will be discussed in section 4.2) sediment pore water was 53.4 times  $\text{CH}_4$   
281 supersaturated; induces significant  $\text{CH}_4$  influx from intertidal & sub-tidal sediment to estuary.  
282 Advective  $\text{CH}_4$  fluxes from intertidal sediment to adjacent estuary were between  $115.81 \pm 31.02$  and  
283  $199.15 \pm 47.89$   $\mu\text{mol m}^{-2} \text{d}^{-1}$ , having maximal postmonsoon and minimal premonsoon periods (Dutta et  
284 al., 2015b) (Fig.4). The peak postmonsoon advective  $\text{CH}_4$  flux may be ascribed to higher pore water  
285  $\text{CH}_4$  concentration as well as specific discharge ( $0.008 \text{ cm min}^{-1}$ ). Diffusive  $\text{CH}_4$  fluxes from estuarine  
286 bottom lying sediment to the water column ranged from  $7.06 \pm 1.95$  to  $10.26 \pm 2.43$   $\mu\text{mol m}^{-2} \text{d}^{-1}$   
287 (Fig.4), having an annual mean of  $8.45$   $\mu\text{mol m}^{-2} \text{d}^{-1}$  (Dutta et al., 2015b). The diffusive fluxes  
288 calculated for this ecosystem were comparatively higher than Yantze estuary ( $1.7 - 2.2$   $\mu\text{mol m}^{-2} \text{d}^{-1}$ )  
289 (Zhang et al. 2008b) but much lower than White Oak river estuary ( $17.1$   $\text{mmol m}^{-2} \text{d}^{-1}$ ) (Kelly et al.  
290 1990). Fluxes were maximal during postmonsoon and minimal during pre-monsoon periods. The peak  
291 postmonsoon diffusive  $\text{CH}_4$  fluxes may be ascribed to maximal pore water  $\text{CH}_4$  concentrations while the  
292 reverse case applies premonsoon.





293 From the methanogenic deep sediment layer the produced  $\text{CH}_4$  partially diffuses upward, which  
294 undergoes aerobic and anaerobic oxidation in sediment before being transported to the forest  
295 atmosphere. But only aerobic  $\text{CH}_4$  oxidation at sediment surface has been included in this study. The  
296 seasonal variation of surface sediment  $\text{CH}_4$  oxidation potentials are presented in Fig.5 and the values  
297 were within the range of that reported for deciduous forest of UK and temperate forests soil in Korea  
298 (Bradford et al. 2001b; Jang et al. 2006). On seasonal basis, the oxidation potential was maximal  
299 premonsoon and minimal monsoon periods having a mean of  $1.758 \pm 0.34 \text{ mg m}^{-2} \text{ d}^{-1}$ . The peak  
300 premonsoon  $\text{CH}_4$  oxidation potential may be due to maximum soil surface temperature (table 1) as  
301 methanotrophy is a microbiological process and rate of any microbiological reaction is directly  
302 proportional with temperature.  $\text{NH}_4^+$  and  $\text{NO}_3^-$  concentrations in mangrove forest sediment surface  
303 varied between  $1.01 - 3.31 \mu\text{M}$  and  $1.11 - 2.98 \mu\text{M}$ , respectively and correlation between  $\text{NH}_4^+$  and  
304  $\text{NO}_3^-$  concentrations vs.  $\text{CH}_4$  oxidation potential ( $[\text{CH}_4]_{(\text{Ox})} = 1.63 - 0.307 [\text{NH}_4^+] + 0.293 [\text{NO}_3^-]$  [ $R^2 =$   
305  $68 \%$ ,  $F = 3.18$ ,  $p = 0.181$ ,  $n = 15$ ]) revealed negative relationship between  $[\text{CH}_4]_{(\text{Ox})}$  and  $[\text{NH}_4^+]$  but  
306 positive with  $[\text{NO}_3^-]$  (table 3). The inhibitory effect of  $[\text{NH}_4^+]$  on  $\text{CH}_4$  oxidation activity may be due to  
307 competition of  $\text{NH}_4^+$  with  $\text{CH}_4$  for the  $\text{CH}_4$  monooxygenases (MMO) in methanotrophic bacteria. Even  
308 though the affinity of MMO for  $\text{CH}_4$  is 600 - to 1300 - fold higher than its affinity for ammonium, high  
309 concentrations of ammonium are known to substantially inhibit the process of methanotrophy in  
310 sediment (Be'dard and Knowles, 1989). Proportional relationship between  $\text{NO}_3^-$  and  $\text{CH}_4$  oxidation may  
311 be related to the demand of type II methanotrophic bacteria for nitrogen sources (Jang et al., 2006).



312 After oxidation the residual diffused CH<sub>4</sub> emits across sediment – atmosphere interface. Monthly  
313 variation of mangrove sediment – atmosphere CH<sub>4</sub> exchange fluxes are presented in Fig.6; having  
314 maximal emission during monsoon and minimal during premonsoon (Dutta et al. 2013). Emission  
315 fluxes estimated for this study point were within the range of that reported for Pichavarm mangrove,  
316 India and mangrove along the south west coast of Puerto Rico (Purvaja et al. 2004; Sotomayor et al.  
317 1994). Mean soil CH<sub>4</sub> emission from this mangrove ecosystem was 7.06 mg m<sup>-2</sup> d<sup>-1</sup>; indicates the  
318 mangrove sediment acts as a rich source of CH<sub>4</sub> to the regional atmosphere. During the observation  
319 period soil temperature (t) ranged between 18.25 ± 0.22 and 28.36 ± 1.02°C and variability of soil CH<sub>4</sub>  
320 emissions (E<sub>M</sub>) were tested statistically with respective ‘t’ and pore water salinity (s). E<sub>M</sub> is best fitted  
321 linearly with ‘t’ and by a second order polynomial equation with ‘s’ as given below:

$$322 \quad E_M = 0.066 t - 1.79 \quad (R^2 = 0.35, F = 5.33, p = 0.041, n = 12)$$

$$323 \quad E_M = 0.0039 s^2 - 0.2006 s + 2.8416 \quad (R^2 = 0.77, F = 7.71, p = 0.029, n = 12)$$

324 The analysis indicates significant correlation between CH<sub>4</sub> fluxes with both the independent variables,  
325 indicating cumulative influences of ‘t’ and ‘s’ on mangrove soil CH<sub>4</sub> emission. Similar phenomenon  
326 was previously reported in Ranong Province mangrove area, Thailand (Lekphet et al. 2005) and a salt  
327 marsh of Queen’s creek (Bartlett et al. 1987). Comparing CH<sub>4</sub> emissions from different littoral zones of  
328 the mangrove forest, higher emissions (0.288 - 0.507 mg m<sup>-2</sup> hr<sup>-1</sup>) were noticed from upper littoral zone  
329 compare to mid & lower littoral zones; may be due to the higher pneumatophore density in that region  
330 (42 number m<sup>-2</sup>) and diffusion of CH<sub>4</sub> through it (Dutta et al. 2013). Mean pneumatophore and



331 bioturbation density in the forest area was counted as  $45 \pm 7$  and  $12 \pm 2$  nos.  $\text{m}^{-2}$ , respectively and  
332 statistical analysis was done in order to examine the influence of pneumatophore and bioturbation on  
333 emission of  $\text{CH}_4$  in this mangrove forest atmosphere. Regression equations between soil  $\text{CH}_4$  emission  
334 rate ( $F_{\text{SA}}$ ) vs. pneumatophores ( $P_{\text{no}}$ ) and bioturbation ( $B_{\text{no}}$ ) density were as follows:

335 
$$F_{\text{SA}} = - 8.59 + 0.330 P_{\text{no}} \text{ (R}^2 = 81.9\%, \text{ F} = 6.94, \text{ p} = 0.032, \text{ n} = 20\text{)}$$

336 
$$F_{\text{SA}} = 6.42 - 0.052 B_{\text{no}} \text{ (R}^2 = 61.9\%, \text{ F} = 5.94, \text{ p} = 0.041, \text{ n} = 20\text{)}$$

337 The statistical analysis revealed significant correlation between dependent & independent variables for  
338 both cases indicating other than physicochemical factors, biological variables (like presence of  
339 pneumatophore and bioturbation) also play a crucial role for  $\text{CH}_4$  emission from the forest sediment.  
340 The positive correlation between sediment  $\text{CH}_4$  emission rate and pneumatophore density indicates  
341 plant mediated emission of  $\text{CH}_4$  in Sundarbans mangrove ecosystem whereas negative correlation with  
342 bioturbation density indicates that burrows favored sediment oxygenation especially in surface layer,  
343 resulting  $\text{CH}_4$  oxidation in surface mangrove sediment and ultimately reduced its emission flux from  
344 sediment. A similar observation on oxidation of surface sediment by crab burrows in the mangrove  
345 environment was previously reported by Kristensen and Alongi, 2006.

346 **4.2 Estuarine  $\text{CH}_4$  cycling:**



347 Physicochemical and biological parameters of the estuarine water column are presented in table – 4 and  
348 on monthly basis from Fig.7A to 7D. For both (temperature and salinity) the values were highest during  
349 the premonsoon and lowest during the postmonsoon (for temperature) and monsoon (for salinity)  
350 months. Marginal variation of temperature and salinity in estuarine surface and bottom water clearly  
351 indicates a vertically well mixed water column. Surface water pH varied over a narrow range ( $8.10 \pm$   
352  $0.03$  to  $8.17 \pm 0.16$ ) and seasonal differences were not significant. Dissolved oxygen (DO)  
353 concentrations in estuarine surface and bottom waters were high ( $6.04 \pm 0.73$  to  $7.27 \pm 1.14$  mg L<sup>-1</sup> and  
354  $5.41 \pm 0.03$  to  $5.98 \pm 0.79$  mg L<sup>-1</sup>, respectively) being maximal during postmonsoon and minimal during  
355 monsoon periods. DO % of saturation varied between 94.8 and 99.3; indicates a well oxygenated water  
356 column that would inhibit the anaerobic microbial metabolism of organic matter within estuarine water  
357 column. The chlorophyll concentration in estuarine surface water ranged from  $3.11 \pm 0.39$  to  $7.88 \pm$   
358  $1.90$  µg L<sup>-1</sup> having highest and lowest concentrations during postmonsoon and monsoon, respectively.  
359 Seasonal trends of chlorophyll concentration mirrored the changes in Secchi disc depth, which ranged  
360 between  $29.7 \pm 7.8$  and  $75.9 \pm 7.7$  cm during the study period. The ratio between primary productivity  
361 and community respiration was <1, indicates the estuary is net heterotrophic in nature.

362 During the observation period estuarine surface and bottom waters dissolved CH<sub>4</sub> concentrations ranged  
363 from  $54.20 \pm 5.06$  to  $90.91 \pm 21.20$  and  $47.28 \pm 12.85$  to  $67.97 \pm 33.12$  nM, respectively (Fig.7E);  
364 having maximal postmonsoon and minimal monsoon periods (table 4) (Dutta et al., 2015b). The CH<sub>4</sub>  
365 concentrations measured in this mangrove dominated estuary was within the range of that measured in



366 Thames estuary, Loire estuary but higher than Hooghly estuary, Yangtze River estuary, Sado estuary  
367 and Elbe estuary (Middelburg et al. 2002; Biswas et al. 2007; Zhang et al. 2008b). The peak  
368 postmonsoon CH<sub>4</sub> concentrations may be attributed to cumulative effect of maximal supply of dissolved  
369 CH<sub>4</sub> rich pore water from intertidal mangrove sediment and minimal CH<sub>4</sub> oxidation (will be discussed  
370 later) in the estuarine water column. Like other tropical, sub-tropical and temperate estuaries (Upstill-  
371 Goddard et al. 2000; Middelburg et al. 2002; Biswas et al. 2007; Zhang et al. 2008b) statistical analysis  
372 revealed significant negative correlation between estuarine dissolved CH<sub>4</sub> levels with respective salinity  
373 (Premonsoon:  $R^2 = 89.1\%$ ,  $F = 49.15$ ,  $p < 0.001$ ,  $n = 8$ ; Monsoon:  $R^2 = 95.2\%$ ,  $F = 120.12$ ,  $p < 0.001$ ,  $n$   
374  $= 8$ ; Postmonsoon:  $R^2 = 75.8\%$ ,  $F = 18.83$ ,  $p = 0.005$ ,  $n = 8$ ) indicating salinity is the major controlling  
375 factor for variability of CH<sub>4</sub> levels in this estuary. Moreover, the stronger degree of correlation during  
376 monsoon months compare to others indicates fresh water runoff mediated addition of CH<sub>4</sub> to the estuary  
377 during this period. Other than salinity, statistically no significant correlation was obtained with other  
378 physicochemical and biological variables ( $[CH_4] = -297 - 0.14 \text{ temperature} + 58 \text{ pH} + 2.69$   
379  $[\text{chlorophyll}] - 19.1 [\text{dissolved oxygen}] + 8.5 (\text{NPP/R})$  [ $R^2 = 75\%$ ,  $F = 1.20$ ,  $p = 0.513$ ,  $n = 24$ ]) (table  
380 5); pointed towards in situ methanogenesis is not occurring within this estuary and estuarine dissolved  
381 CH<sub>4</sub> is entirely exogenous in nature (Dutta et al., 2015b).

382 Being well oxygenated, the water column presumably restrained methanogenesis but induced  
383 methanotrophy. CH<sub>4</sub> oxidation in the subsurface water was studied based on time dependent CH<sub>4</sub>  
384 reduction in the incubated samples and during this experiment none of the samples showed time series



385 increment of CH<sub>4</sub> concentration i.e. net CH<sub>4</sub> production. Specific rate of CH<sub>4</sub> oxidation (0.009 ± 0.001  
386 to 0.018 ± 0.001 hr<sup>-1</sup>) and consumption (0.54 ± 0.12 to 1.26 ± 0.27 nmol L<sup>-1</sup> hr<sup>-1</sup>) in estuarine surface  
387 water was distinctly seasonal; having maximal premonsoon and minimal postmonsoon periods (Fig.7F).  
388 The mean dissolved CH<sub>4</sub> consumption rate was 20.59 nmol L<sup>-1</sup> d<sup>-1</sup>, about 8.11 times lower than rate of  
389 CH<sub>4</sub> oxidation reported in the freshwater region of the Hudson estuary during summer (167 nmol L<sup>-1</sup> d<sup>-1</sup>  
390 <sup>1</sup>) (De Angelis and Scranton 1993). Aquatic CH<sub>4</sub> oxidation is a microbial process, so, the  
391 physicochemical parameters like temperature (thermal), salinity (tonicity), oxygen (oxidative), DIN  
392 (nutrient) and turbidity (surface) may have significant metabolic effects in this process. Moreover, other  
393 biological processes like primary production and community respiration may be considered to be  
394 influencing for this microbial process. Influence of salinity on dissolved CH<sub>4</sub> oxidation rate has been  
395 reported previously by de Angelis & Scranton 1993. According to their observation in Hudson estuary,  
396 high oxidation rates (4 to 167 nmol L<sup>-1</sup> d<sup>-1</sup>) were found only at salinities below 6, rates at higher  
397 salinities being 1 to 2 orders of magnitude lower. The value for dissolved O<sub>2</sub> was significantly above the  
398 range of the estimated half-saturation constant for CH<sub>4</sub> oxidation, K<sub>m</sub> (0.5 - 0.8 mg L<sup>-1</sup>; Lidstrom and  
399 Somers 1984) or the reported optimum range of 0.1-1.0 mg L<sup>-1</sup> (Rudd and Hamilton 1975) for microbial  
400 CH<sub>4</sub> oxidation in the water column. Influences of dissolved inorganic nitrogen (DIN) concentration on  
401 microbial CH<sub>4</sub> oxidation had been reported previously in Lake 227 (Rudd and Hamilton 1979).  
402 According to their observation in the presence of O<sub>2</sub> concentrations > 31 μM bacterial CH<sub>4</sub> oxidation  
403 was inhibited when DIN concentration was low (< 3 μM) as methanotrophs can fix nitrogen under low



404 DIN conditions ( $< 3\mu\text{M}$ ). The nitrogen fixation is disrupted by high concentrations of  $\text{O}_2$  but not  
405 inhibited when DIN concentration reaches to  $20\ \mu\text{M}$ . Moreover, turbid condition of the estuary  
406 methanotrophs associated with particulate matter can encounter high dissolved  $\text{CH}_4$  levels in estuarine  
407 water column (Abil et al. 2007).

408 A multiple regression analysis was done in order to point out key controlling factor for  $\text{CH}_4$  oxidation in  
409 this mangrove dominated estuary. Here the dependent variable is dissolved  $\text{CH}_4$  oxidation rate  
410 ( $[\text{CH}_4]_{\text{DOX}}$ ) and independent variables are water temperature (T), salinity (S), dissolved oxygen (DO),  
411 dissolved inorganic nitrogen (DIN), net heterotrophy (R/P) and secchi disc depth ( $S_d$ ). The resultant  
412 regression equation between these variables ( $[\text{CH}_4]_{\text{DOX}} = - 65.9 + 0.756 T - 2.18 S + 7.53 \text{ DO} - 0.408$   
413  $\text{DIN} - 2.01 \text{ P/R} - 0.304 S_d$  [ $R^2 = 91.6\%$ ,  $F = 9.12$ ,  $p = 0.014$ ,  $n = 12$ ]) revealed significant correlation  
414 between  $[\text{CH}_4]_{\text{DOX}}$  with S, DO &  $S_d$  (table 6); indicating cumulative influence of these variables on  
415 variability of  $[\text{CH}_4]_{\text{DOX}}$  in this estuarine water.

416 In a study of  $\text{CH}_4$  oxidation in a freshwater lake, Panganiban et al. 1979 reported that 30-60% of the  
417  $\text{CH}_4$  oxidized was incorporated with the cell under aerobic conditions but essentially none was  
418 incorporated under anaerobic conditions. Rudd and Taylor, 1980 reported an incorporation percentage  
419 of 50% in a study of  $\text{CH}_4$  oxidation in a freshwater lake. In the mangrove dominated estuary of  
420 Sundarbans, the  $\text{CH}_4$  oxidation in the water column progressed at aerobic conditions. Assuming that 30-  
421 50% of the  $\text{CH}_4$  carbon oxidized by methanotrophs was converted to organic matter (bacterial cell  
422 materials) and the remainder to  $\text{CO}_2$ . The mean  $\text{CH}_4$  carbon converted to bacterial cell material was



423 computed as  $0.59 \text{ mg C m}^{-2} \text{ d}^{-1}$  while primary productivity mediated production of organic carbon was  
424  $1545 \text{ mg C m}^{-2} \text{ d}^{-1}$ . Thus, the production of organic carbon as a result of  $\text{CH}_4$  oxidation was only  
425 0.038% of that generated by primary production at that time. The remaining oxidised  $\text{CH}_4$  is  
426 quantitatively converted to less radiatively active  $\text{CO}_2$  & plays a crucial role in the estuarine carbon  
427 cycle. Using the stoichiometric equation for aerobic  $\text{CH}_4$  oxidation mechanism,  $\text{CH}_4$  oxidation mediated  
428  $\text{CO}_2$  production rate in this mangrove dominated estuary was  $3.25 \text{ mg m}^{-2} \text{ d}^{-1}$ . Extrapolating the value  
429 for entire Sundarbans estuaries, total  $\text{CO}_2$  production from  $\text{CH}_4$  oxidation mechanism was  $2.13 \text{ Gg yr}^{-1}$ .

430 Surface water  $\text{CH}_4$  % of saturation was ranged from  $2483.02 \pm 950.18$  to  $3525.45 \pm 1053.72$ ; indicating  
431 the estuarine water was  $\text{CH}_4$  supersaturated inducing  $\text{CH}_4$  exchange across water – atmosphere  
432 interface. Monthly variation of air – water  $\text{CH}_4$  flux and  $\text{CH}_4$  concentration in estuarine surface water  
433 are presented graphically in Fig.7E. Air – water  $\text{CH}_4$  fluxes from this estuary ranged between  $6.27 \pm$   
434  $1.61$  and  $10.67 \pm 6.92 \text{ } \mu\text{mol m}^{-2} \text{ d}^{-1}$ ; having minimal premonsoon and maximal monsoon periods (Dutta  
435 et al., 2015b). Minimal premonsoon  $\text{CH}_4$  fluxes may be attributed to the lowest value of wind speed  
436 over the estuary as well as surface water dissolved  $\text{CH}_4$  levels. Flux values estimate for this site fall  
437 within the range measured in the Hooghly estuary ( $0.88 - 148.63 \text{ } \mu\text{mol m}^{-2} \text{ d}^{-1}$ ) (Biswas et al. 2007) but  
438 are much lower than those reported for some other estuaries like Oregon estuary ( $181.3 \text{ } \mu\text{mol m}^{-2} \text{ d}^{-1}$ )  
439 (De Angelis and Lilley, 1987). The large variation in water – atmosphere  $\text{CH}_4$  flux between different  
440 estuaries reflects a combination of dissolved  $\text{CH}_4$  concentration, the gas transfer velocity and variability  
441 of estuarine regimes (Dutta et al., 2015b). Wind speed over the estuarine water surface ranged between





442  $2.28 \pm 1.01$  and  $3.16 \pm 1.79 \text{ ms}^{-1}$ . The value seems to be low; may be due to high resistance offered by  
443 the mangrove vegetation resulting low gas transfer velocity as well as air - water  $\text{CH}_4$  exchange flux  
444 value in this estuary. Our flux estimates were analyzed statistically to examine the influence of  
445 temperature and salinity on their variability. In both cases the analysis revealed significant correlations  
446 (water temperature:  $R^2 = 61\%$ ,  $F = 6.71$ ,  $p = 0.029$ ,  $n = 24$ ; salinity:  $R^2 = 54\%$ ,  $F = 5.31$ ,  $p = 0.037$ ,  $n =$   
447  $24$ ) indicating a cumulative effect of temperature and salinity on estuarine  $\text{CH}_4$  emission (Dutta et al.,  
448 2015b).

#### 449 **4.3. Atmospheric $\text{CH}_4$ dynamics:**

450 Temperature of the mangrove forest atmosphere varied between  $17.34 \pm 4.0$  to  $30.34 \pm 0.91^\circ\text{C}$  at 10 m  
451 and  $16.17 \pm 1.80$  to  $29.73 \pm 1.13^\circ\text{C}$  at 20 m; being maximal premonsoon and minimal postmonsoon  
452 seasons (table 7). Wind velocity varied between  $0.41 \pm 0.36$  and  $1.32 \pm 1.11 \text{ m s}^{-1}$  at 10 m height and  
453  $0.80 \pm 0.88$  to  $1.64 \pm 1.37 \text{ m s}^{-1}$  at 20 m height; having maximal monsoon and minimal postmonsoon  
454 periods. The atmospheric turbulence expressed by friction velocity ( $U^*$ ) plays an important role in  
455 controlling the stability of the atmosphere & varied between  $0.01$  and  $1.2 \text{ m s}^{-1}$ . Planetary boundary  
456 layer or atmospheric boundary layer (PBL) height over the mangrove forest atmosphere varied between  
457  $702.45 \text{ m}$  and  $936.59 \text{ m}$ ; having maximal height during premonsoon and minimal during monsoon  
458 periods. Mean atmospheric boundary layer height over the tropical mangrove forest atmosphere was  
459  $811.7 \text{ m}$  on annual basis. Values of other micrometeorological indices such as drag coefficient and



460 roughness height are presented in table 5. The seasonal variation for drag co-efficient may be attributed  
461 to the variation of wind speed in this mangrove forest atmosphere (Smith and Banke, 1975) while the  
462 values for both drag coefficient and roughness height were minimum in monsoon period. The low  
463 values of drag coefficient and roughness length could be deemed specific for this particular surface  
464 which is due to the action of low - pressure force on individual surface elements and the low shearing  
465 stress generated by particular wind (Mukhopadhyay et al., 2002).

466 Monthly variation of CH<sub>4</sub> mixing ratio at 10 & 20 m heights of the forest atmosphere are presented in  
467 Fig.8A; indicating minimal premonsoon (at both 10 and 20 m heights) and maximal during monsoon  
468 and postmonsoon periods for 10 m and 20 m heights, respectively (table 7). The maximal monsoon CH<sub>4</sub>  
469 mixing ratio at 10 m height may be attributed to maximum monsoon CH<sub>4</sub> emission from sediment and  
470 aquatic surfaces and primarily it's mixing to the lower atmosphere of the mangrove ecosystem. Diurnal  
471 variation of CH<sub>4</sub> in the mangrove forest atmosphere at 10 m and 20 m heights in a month of January is  
472 presented in Fig.8B; indicating peak concentrations during early morning may be attributed to CH<sub>4</sub>  
473 accumulation within a stable boundary layer in that period (Dutta et al., 2013c). With progress of the  
474 day due to increment of atmospheric turbulence the stable layer breaks up resulting decrease of CH<sub>4</sub>  
475 concentration in the lower atmosphere (Mukhopadhyay et al. 2002). Changes in the  
476 micrometeorological parameters at the study site change the stability (Z/L) of the atmosphere, which in  
477 turn may alter the atmospheric CH<sub>4</sub> mixing ratio in the lower atmosphere ([CH<sub>4</sub>]<sub>10m</sub>). Statistical analysis  
478 revealed significant correlation between Z/L and [CH<sub>4</sub>]<sub>10m</sub> ([CH<sub>4</sub>]<sub>10m</sub> = 2.56 + 2.25 Z/L [R<sup>2</sup> = 74.8%, p



479 < 0.001,  $F = 29.73$ ,  $n = 30$ ]); indicates potential impact of micrometeorological parameters on  
480 variability of  $\text{CH}_4$  mixing ratio at lower atmosphere. Comparing  $\text{CH}_4$  distribution along vertical column  
481 of the forest atmosphere it was evident that  $\text{CH}_4$  mixing ratio at 10 m height was 1.02 times higher than  
482 20 m height; induces biosphere – atmosphere  $\text{CH}_4$  exchange in this mangrove environment depending  
483 upon micrometeorological conditions of the atmosphere. Monthly variation of biosphere – atmosphere  
484  $\text{CH}_4$  exchange flux is presented in Fig.8C having maximal flux monsoon and minimal postmonsoon  
485 periods. This mangrove biosphere acts as a source for  $\text{CH}_4$  during monsoon, when  $\Delta\chi$  is significantly  
486 positive and as sink during pre and post monsoon seasons, when  $\Delta\chi$  is negative. The contributory  
487 processes to the  $\Delta\chi$  are emission from water and soil resulting enrichment in the 10 m layer and  
488 oxidation (both microbial and photochemical) causing depletion at 10 and 20 m, respectively (Dutta et  
489 al. 2013). Mean biosphere – atmosphere methane exchange flux was calculated as  $0.086 \text{ mg m}^{-2} \text{ d}^{-1}$ ;  
490 indicates on annual mean basis the mangrove ecosystem acts as a source of  $\text{CH}_4$  to the upper  
491 atmosphere. Mean compensation point (i.e. where net biosphere - atmosphere  $\text{CH}_4$  flux is zero) for  $\text{CH}_4$   
492 in this subtropical mangrove forest was 1.997 ppmv. Statistical analysis was done between biosphere –  
493 atmosphere  $\text{CH}_4$  flux ( $F_{\text{BA}}$ ) and sensible heat flux ( $H$ ) as the transport of energy and mass are partially  
494 controlled by ‘ $H$ ’. The regression equation [ $F_{\text{BA}} = - 0.0013 H^2 + 0.0967 H + 0.7789$  ( $R^2 = 0.53$ ,  $F =$   
495  $7.72$ ,  $p = 0.002$ ,  $n = 12$ )] explains 53% variability between dependent & independent variables  
496 indicating significant influence of sensible heat flux on variability of biosphere – atmosphere  $\text{CH}_4$   
497 exchange in this tropical mangrove forest ecosystem.



498 On annual basis mean daytime CH<sub>4</sub> mixing ratio was 1.03 times lower than night-time; the variability is  
499 presumed to be governed by photo-oxidation and diurnal changes in the boundary layer height. But  
500 statistically no significant correlation was obtained between variability of daytime and nighttime CH<sub>4</sub>  
501 mixing ratio with PBL height ( $\Delta\text{CH}_4 = -0.0118\Delta\text{PBL} + 0.3045$ ,  $R^2 = 16.2\%$ ,  $F = 0.321$ ,  $p = 0.987$ ,  $n =$   
502  $12$ ); indicating variability of atmospheric boundary layer height was not the major controlling factor for  
503  $\Delta\text{CH}_4$ , that pointed towards large atmospheric CH<sub>4</sub> photo-oxidation in the mangrove forest atmosphere.  
504 CH<sub>4</sub> photo-oxidation rate in this subtropical mangrove forest atmosphere varied between  $6.05 \times 10^{10}$  and  
505  $1.67 \times 10^{11}$  molecules  $\text{cm}^{-3} \text{d}^{-1}$  being maximum oxidation during monsoon and minimum during  
506 postmonsoon periods (Dutta et al. 2015c). The peak monsoon CH<sub>4</sub> photo-oxidation rate may be  
507 attributed to maximum CH<sub>4</sub> supply through emission as well as high UV index and UV erythermal dose  
508 irradiance during this period in these subtropical latitudes (Panicker et al. 2014). Considering the mean  
509 day light period as 12 hours and  $6.023 \times 10^{23}$  molecules equals to 1 mole or 16000 mg CH<sub>4</sub>, the mean  
510 CH<sub>4</sub> photo-oxidation rate in this tropical mangrove forest atmosphere was calculated as  $3.25 \times 10^{-9}$  mg  
511  $\text{cm}^{-3} \text{d}^{-1}$ .

#### 512 **4.4: Quantitative CH<sub>4</sub> budget from Indian Sundarbans:**

513 A box diagram (fig.9) was constructed for describing biogeochemical CH<sub>4</sub> cycling in Sundarbans  
514 biosphere reserve. In the model different subsystems are designated as separate reservoir. CH<sub>4</sub> storage in  
515 each reservoir and exchange fluxes of CH<sub>4</sub> between different reservoirs are presented as an annual mean



516 and values were used to calculate the input and output of CH<sub>4</sub> to/from the reservoirs, which in turn  
517 established the CH<sub>4</sub> budget for this mangrove-dominated estuarine system.

518 **Mangrove sediment methane budget:**

- 519 1. Mean CH<sub>4</sub> production potential in intertidal forest sediment (up to the depth of 25 cm) was 3547  
520  $\mu\text{mol m}^{-3} \text{d}^{-1}$ . Considering the rate equal to in situ CH<sub>4</sub> production and extrapolating over entire  
521 forest, total CH<sub>4</sub> production within 25 cm depth of the forest sediment is 21.75 Ggyr<sup>-1</sup>.
- 522 2. Intertidal sediment pore water CH<sub>4</sub> concentration was 3451 nM and extrapolating the  
523 concentration for entire mangrove forest (up to 25 cm depth), the sediment stands as a reservoir  
524 pool of 0.031Gg CH<sub>4</sub>.
- 525 3. The intertidal sediment pore water methane concentration was about 55 times supersaturated  
526 than adjacent estuarine water (63.04 nM) indicating significant out - flux of CH<sub>4</sub> rich pore water  
527 from intertidal sediment to estuary during low tide phase via advective transport.
- 528 4. About 8.2% of the produced CH<sub>4</sub> is advectively transported to the adjacent estuarine system with  
529 a rate of 159.52  $\mu\text{mol m}^{-2} \text{d}^{-1}$ .
- 530 5. Mean CH<sub>4</sub> oxidation potential at intertidal forest sediment surface was 1.758  $\text{mg m}^{-2} \text{d}^{-1}$  and  
531 total oxidation was 2.70 Ggyr<sup>-1</sup>, when extrapolated for entire forest area of Sundarbans. The



532 value indicates only 12.41% of produced CH<sub>4</sub> is oxidized at sediment surface; presenting petite  
533 activity of methanotrophs in comparison to the methanogens in forest sediment.

534 6. Total CH<sub>4</sub> emission across sediment – atmosphere interface of the mangrove forest was 10.8  
535 Ggyr<sup>-1</sup> (about 49.6% of total produced CH<sub>4</sub> in sediment) with a rate of 7.06 mg m<sup>-2</sup> d<sup>-1</sup>.

536 7. The total CH<sub>4</sub> emission and oxidation from/at the mangrove surface sediment was 6.05 and 1.51  
537 times higher, respectively compare to total CH<sub>4</sub> advectively transported to the estuary; indicates  
538 emission acts as major CH<sub>4</sub> removal pathway from intertidal mangrove sediment.

539 8. Balancing total production and removal, annually 6.46 GgCH<sub>4</sub> remains unexplained. This  
540 establishes the existence of anaerobic methane oxidation in mangrove sediment column which  
541 was not covered in this study.

#### 542 **Sub-tidal sediment CH<sub>4</sub> budget:**

543 1. CH<sub>4</sub> production potential of 0 – 5 cm depth of estuarine underlying sediment (sub-tidal  
544 sediment) was 48.88 μmol m<sup>-3</sup> d<sup>-1</sup> and total production was 0.026 Ggyr<sup>-1</sup> when extrapolated for  
545 entire sub-tidal area for estuaries of Sundarbans.

546 2. Mean sub-tidal sediment (0 – 5 cm) pore water CH<sub>4</sub> concentration was 3286 nM; which was  
547 about 52.13 times supersaturated than overlying estuarine water inducing diffusive CH<sub>4</sub> transport  
548 from sub-tidal sediment to the overlying estuary.



549        3. Mean diffusive CH<sub>4</sub> flux from sub-tidal sediment to the overlying estuary was 8.45 μmol m<sup>-2</sup> d<sup>-1</sup>.  
550            Extrapolating the rate for entire sub-tidal area of Sundarbans, the sub-tidal sediment acts as a  
551            source of 0.089 GgCH<sub>4</sub> annually to the upper estuarine system.

552    **Estuarine CH<sub>4</sub> budget:**

553        1. Total CH<sub>4</sub> input from sediment to estuary (by both advection and diffusion transports) was  
554            1.875Gg yr<sup>-1</sup>. Advective flux being 20 times higher than diffusive flux acts as major source for  
555            CH<sub>4</sub> to the estuary.

556        2. Mean dissolved CH<sub>4</sub> concentration in the estuary was 63.04 nM. Extrapolating this over the  
557            entire volume of the estuaries of the Sundarbans, the system stands as a reserve pool of 0.011Gg  
558            CH<sub>4</sub> (Dutta et al., 2015b).

559        3. The total CH<sub>4</sub> oxidation rate in the estuarine water column was 1.30Ggyr<sup>-1</sup> with a rate of 20.59  
560            nmol L<sup>-1</sup> d<sup>-1</sup>.

561        4. Mean CH<sub>4</sub> emission flux across the water - atmosphere interface of the estuary was 8.88 μmol m<sup>-2</sup>  
562            d<sup>-1</sup>. Extrapolating this over the total estuarine surface area, on an annual basis the mangrove  
563            associated estuaries of the Sundarbans are a source of 0.093Gg CH<sub>4</sub> to the regional atmosphere,  
564            which is only 4.96 % of total CH<sub>4</sub> supplied to the estuary.



- 565 5. CH<sub>4</sub> oxidation, being 14 times higher than water - atmosphere exchange, is considered as  
566 principal CH<sub>4</sub> removal mechanism in this estuary.
- 567 6. Mean turnover time of CH<sub>4</sub> in the water column relative to oxidation and emission was 3.77  
568 days, which is in the range of turnover times relative to oxidation reported for the low salinity  
569 region of the Hudson estuary (1.4 – 9 days) (De Angelis and Scranton 1993).
- 570 7. The total sink of CH<sub>4</sub> due to these oxidation and emission processes were 1.39 Ggyr<sup>-1</sup>, about  
571 74.13 % of total CH<sub>4</sub> supply to the estuary, indicating a significant export flux of CH<sub>4</sub> from  
572 estuary to the adjacent continental shelf.
- 573 8. Balancing CH<sub>4</sub> sources vs. sinks in this estuarine system, the export flux of CH<sub>4</sub> from estuary to  
574 the continental shelf was 0.485 Ggyr<sup>-1</sup>, indicating a significant contribution from the Sundarbans  
575 estuaries to the CH<sub>4</sub> budget of the northern Bay of Bengal (Dutta et al., 2015b).

576 **Atmospheric CH<sub>4</sub> budget:**

- 577 1. Net CH<sub>4</sub> emission from Sundarbans mangrove ecosystem (sediment & estuarine surfaces) to the  
578 regional atmosphere was 10.89 Ggyr<sup>-1</sup>, of which sediment is the principal contributor (99.17%).
- 579 2. Comparison to the global mean CH<sub>4</sub> emission rate from mangrove forest & creeks (10.76 mg m<sup>-2</sup>  
580 d<sup>-1</sup>; Barnes et al., 2006) mean CH<sub>4</sub> emission rate from Sundarbans mangrove environment is





581 approximately 2.99 times lower; representing partial impact of this mangrove system towards  
582 earth's global warming as well as climate change scenario.

583 3. Atmospheric CH<sub>4</sub> mixing ratio in 10 m and 20 m heights of the forest atmosphere were 2.038  
584 and 1.987 ppmv, respectively having mean of 2.013 ppmv. Extrapolating over entire Sundarbans  
585 up to the height of atmospheric boundary layer (811.7 m), atmosphere stands as a reservoir pool  
586 of 11.2 GgCH<sub>4</sub>.

587 4. The annual mean mangrove biosphere atmosphere CH<sub>4</sub> exchange flux was 0.086 mg m<sup>-2</sup> d<sup>-1</sup> and  
588 the former when multiplied by the total forest area of the Sundarbans yields that this tropical  
589 mangrove ecosystem annually acts as source for 0.30 GgCH<sub>4</sub> to the regional atmosphere (about  
590 2.75% of total CH<sub>4</sub> input from water & sediment surfaces).

591 5. Total CH<sub>4</sub> photo-oxidation in the forest atmosphere up to height of atmospheric boundary layer  
592 was 9.26 Ggyr<sup>-1</sup> with a mean rate of 3.25 x 10<sup>-9</sup> mg cm<sup>-3</sup> d<sup>-1</sup>. Compare to total CH<sub>4</sub> supply to the  
593 forest atmosphere, about 85% is photo-oxidized within atmospheric boundary layer of  
594 Sundarbans and is recognized as major atmospheric CH<sub>4</sub> removal pathway. The photo-oxidation  
595 mediated depletion of CH<sub>4</sub> is highly significant in atmospheric chemistry producing byproducts  
596 like HCHO, O<sub>3</sub> depending upon ambient NO<sub>x</sub> level. Balancing total atmospheric sources and  
597 sinks, annually 1.33Gg CH<sub>4</sub> remains unbalanced in the atmosphere, which enriches regional  
598 atmospheric CH<sub>4</sub> mixing ratio.

## 599 **5. Conclusion:**



600 CH<sub>4</sub> production potential within 25 cm depth of the forest sediment is 21.75 Ggyr<sup>-1</sup> and pore water CH<sub>4</sub>  
601 concentration was 3541 nM. CH<sub>4</sub> fluxes across intertidal sediment – atmosphere interface acts as major  
602 sink for produced CH<sub>4</sub> in intertidal sediment over surface layer CH<sub>4</sub> oxidation and advective CH<sub>4</sub>  
603 transport to estuary. The process of methanogenesis is totally restricted within estuarine water column  
604 and is supplied from adjacent mangrove forest ecosystem and underlying sediment of the estuary.  
605 Advective flux being 20 times higher than diffusive flux acts as major source for CH<sub>4</sub> to the estuary.  
606 CH<sub>4</sub> oxidation, being 14 times higher than water - atmosphere exchange, is considered the principal  
607 CH<sub>4</sub> removal mechanism in this estuary. Total annual CH<sub>4</sub> emission from sediment and water surfaces  
608 of the Sundarbans mangrove biosphere was 10.89Gg, of which sediment is the principal contributor  
609 (99.17%). Compare to total CH<sub>4</sub> supply to the atmosphere, about 85% is photo-oxidized within  
610 atmospheric boundary layer of Sundarbans and 2.75% is transported to the upper atmosphere through  
611 biosphere – atmosphere CH<sub>4</sub> exchange flux.

## 612 **6. Acknowledgement:**

613 The authors thank the Ministry of Earth Science, Govt. of India sponsored Sustained Indian Ocean  
614 Biogeochemistry and Ecological Research (SIBER) programme for partial financial support to carry out  
615 the study. We are thankful to the Sundarbans Biosphere Reserve for extending necessary help and  
616 support for conducting fieldwork and measurements related to the study.

## 617 **7. References:**



- 618 Abril, G., Commarieu, M.V., Gue´rin, F.: Enhanced methane oxidation in an estuarine turbidity  
619 maximum. *Limnol. Oceanogr.* 52(1), 470 – 475, 2007.
- 620 Barnes, J., Ramesh, R., Purvaja, R., Nirmal Rajkumar, A., Senthil Kumar, B., Krithika, K.,  
621 Ravichandran, K., Uher, G., Upstill-Goddard, R.: Tidal dynamics and rainfall control N<sub>2</sub>O and CH<sub>4</sub>  
622 emissions from a pristine mangrove creek. *Geophys. Res. Lett.* 33, L15405, 2006.
- 623 Barrett K.: Oceanic ammonia emissions in Europe and their transboundary fluxes. *Atmospheric*  
624 *Environment* 32, 381 – 391, 1998.
- 625 Bartlett, K. B., Bartlett, D. S., Harris, R. C., Sebacher, D. I.: Methane emissions along a salt marsh  
626 gradient. *Biogeochemistry* 4, 183-202, 1987.
- 627 Be´dard, C., Knowles, R., 1989. Physiology, biochemistry, and specific inhibitors of CH<sub>4</sub>, NH<sub>4</sub><sup>+</sup>, and  
628 CO oxidation by methanotrophs and nitrifiers. *Microbiol. Rev.* 53, 68–84.
- 629 Biswas, H., Mukhopadhyay, S.K., Sen, S., Jana, T.K.: Spatial and temporal patterns of methane  
630 dynamics in the tropical mangrove dominated estuary, NE Coast of Bay of Bengal, India. . *J. Mar. Syst.*  
631 68, 55–64, 2007.



- 632 Bouillon, S., Middelburg, J.J., Dehairs, F., Borges, A.V., Abril, G., Flindt, M.R., Ulomi, S., Kristensen,  
633 E.: Importance of intertidal sediment processes and porewater exchange on the water column  
634 biogeochemistry in a pristine mangrove creek (Ras Dege, Tanzania). *Biogeosciences* 4, 311-322, 2007c.
- 635 Bradford, M.A., Ineson, P., Wookey, P.A., Lappin-Scott, H.M.: The effects of acid nitrogen and acid  
636 sulphur deposition on CH<sub>4</sub> oxidation in a forest soil: a laboratory study. *Soil Biol Biochem* 33,1695 –  
637 1702, 2001b.
- 638 Canfield, D. E., Kristensen, E., Thamdrup, B.O.: The sulfur cycle. *Advanced Marine Biology* 48, 313 –  
639 381, 2005.
- 640 De Angelis, M.A., Scranton, M.I.: Fate of methane in the Hudson River and estuary. *Glob.*  
641 *Biogeochem. Cycles* 7, 509 –523, 1993.
- 642 De Angelis, M.A., Lilley, M.D.: Methane in surface waters of Oregon estuaries and rivers. *Limnol.*  
643 *Oceanogr.* 32, 716 –722, 1987.
- 644 Dutta, M.K, Ray, R., Mukherjee, R., Jana, T.K., Mukhopadhyay, S.K.: Atmospheric fluxes and photo-  
645 oxidation of methane in the mangrove environment of the Sundarbans, NE coast of India; A case study  
646 from Lothian Island. *Agricultural and Forest Meteorology*, 213, 33 – 41, 2015c.



- 647 Dutta, M.K., Mukherkjee, R., Jana, T.K., Mukhopadhyay, S.K.: Biogeochemical dynamics of  
648 exogenous methane in an estuary associated to a mangrove biosphere; the Sundarbans, NE coast of  
649 India. *Marine Chemistry* 170, 1 – 10, 2015b.
- 650 Dutta, M.K., Chowdhury, C., Jana, T.K., Mukhopadhyay, S.K.: Dynamics and exchange fluxes of  
651 methane in the estuarine mangrove environment of Sundarbans, NE coast of India. *Atmos. Environ.* 77,  
652 631-639, 2013.
- 653 Ding, W., Cai, Z., Tsuruta, H., Li, X.: Key factors affecting spatial variation of methane emissions  
654 from freshwater marshes. *Chemosphere* 51, 167–173, 2003.
- 655 Ehhalt D.H., Rohrer, F.: Dependence of the OH concentration on solar UV. *Journal of Geophysical*  
656 *Research*, 105, 3565-3571, 2009.
- 657 Frankignoulle, M., Borges, A.V.: Direct and indirect pCO<sub>2</sub> measurements in a wide range of pCO<sub>2</sub> and  
658 salinity values (the Scheldt estuary), *Aquat. Geochem.* 7, 267–273, 2001.
- 659 Ganguly D., Dey, M., Mandal, S.K., De, T.K., Jana, T.K.: Energy dynamics and its implication to  
660 biosphere-atmosphere exchange of CO<sub>2</sub>, H<sub>2</sub>O and CH<sub>4</sub> in a tropical mangrove forest canopy.  
661 *Atmospheric Environment*, 42, 4172 – 4184, 2008.
- 662 Grasshoff, K., Ehrhardt, M., Kremling, K.: *Methods of seawater analysis*, 2<sup>nd</sup> edition. Germany, 1983.



- 663 Hanson, R.S., Hanson, T.E.: Methanotrophic bacteria. *Micro. and Mole. Bio. Rev.* 60, 439-471, 1996.
- 664 Hoehler, T.M., Alperin, M.J.: Biogeochemistry: Methane minimalism. *Nature* 507, 436 – 437, 2014.
- 665 IPCC, 2007. Summary for policymakers. In: Solomon, S., et al. (Ed.), *Climate Change*  
666 2007: the Physical Science Basis. Contribution of Working Group I to the Fourth Assessment  
667 Report of the Intergovernmental Panel on Climate Change. Cambridge University  
668 Press, Cambridge.
- 669 Jang, I., Lee, S., Hong, J., Kang, H.: Methane oxidation rates in forest soils and their controlling  
670 variables: a review and a case study in Korea. *Ecol Res*, 21, 849–854, 2006.
- 671 Kankaala, P., Huotari, J., Peltomaa, E., Saloranta, T., Ojala, A.: Methanotrophic activity in relation to  
672 methane efflux and total heterotrophic bacterial production in a stratified, humic, boreal lake. *Limnol.*  
673 *Oceanogr.* 51, 1195–1204, 2006.
- 674 Kelley, C.A., Martens, C.S., Chanton, J.P.: Variations in sedimentary carbon remineralization rates in  
675 the White Oak River estuary, North Carolina. *Limnol. Oceanogr.* 35, 372–383, 1990.
- 676 Keller, J. K., Takagi, K. K.: Solid-phase organic matter reduction regulates anaerobic decomposition in  
677 bog soil. *Ecosphere*, 4, 54, 2003.



- 678 Knab, N. J., Cragg, B.A., Hornibrook, E.R.C., Holmkvist, L., Pancost, R.D., Borowski, C., Parkes, R.J.,  
679 Jørgensen, B.B.: Regulation of anaerobic methane oxidation in sediments of the Black Sea.  
680 *Biogeosciences*, 6, 1505–1518, 2009.
- 681 Kristensen, E., Flindt, M.R., Ulomi, S., Borges, A.V., Abril, G., Bouillon, S.: Emission of CO<sub>2</sub> and CH<sub>4</sub>  
682 to the atmosphere by sediments and open waters in two Tanzanian mangrove forests. *Mar. Ecol. Prog.*  
683 *Ser.* 370, 53–67, 2008.
- 684 Kristensen, E., Alongi, D.M.: Control by fiddler crabs (*Uca vocans*) and plant roots (*Avicennia marina*)  
685 on carbon, iron, and sulfur biogeochemistry in mangrove sediment. *Limnology and Oceanography*,  
686 51(4), 1557–1571, 2006.
- 687 Lekphet, S., Nitorisavut, S., Adsavakulchai, S.: Estimating methane emissions from mangrove area in  
688 Ranong Province, Thailand. *Songklanakarin J. Sci. Technol.*, 27(1), 153-163, 2005.
- 689 Lelieveld, J., Crutzen, P.J., Dentener, F.J., Changing concentration, lifetime and climate forcing of  
690 atmospheric methane. *Tellus 50B*, 128–150, 1993.
- 691 Lidstrom, M. E., Somers, L.: Seasonal study of methane oxidation in Lake Washington. *Appl. Environ.*  
692 *Microbiol.* 47, 1255-1260, 1984.



- 693 Liss, P.S., Merlivat, L.: Air sea gas exchange rates: introduction and synthesis. In: Buat-Menard, P.  
694 (Ed.), *The Role of Air Sea Exchange in Geochemical Cycling*. D. Reidel, Hingham, MA, 113 – 129,  
695 1986.
- 696 Lu, C.Y., Wong, Y.S., Tam, N.F.Y., Ye, Y., Lin, P.: Methane flux and production from sediments of a  
697 mangrove wetland on Hainan Island China. *Mangroves Salt Marshes*, vol. 3, no. 1, p. 41-49, 1999.
- 698 Mayumi, D., Mochimaru, H., Yoshioka, H., Sakata, S., Maeda, H., Miyagawa, Y.: Evidence for  
699 syntrophic acetate oxidation coupled to hydrogenotrophic methanogenesis in the high-temperature  
700 petroleum reservoir of Yabase oil field (Japan). *Environ. Microbiol.* 13, 1995–2006, 2011.
- 701 Mukhopadhyay S.K., Biswas, H., De, T.K., Sen, S., Sen, B.K., Jana, T.K.: Impact of Sundarbans  
702 mangrove biosphere on the carbon dioxide and methane mixing ratio at the NE coast of Bay of Bengal,  
703 India. *Atmospheric Environment* 36 (4), 629–638, 2002.
- 704 Megonigal, J.P., Hines, M.E., Visscher, P.T.: Anaerobic metabolism: linkages to trace gases and aerobic  
705 processes. In *Biogeochemistry*. Ed. W.H. Schlesinger. Elsevier-Pergamon, Oxford, 317– 424, 2004.
- 706 Middelburg, J.J., Nieuwenhuize, J., Iversen, N., Hoegh, N., DeWilde, H., Helder, W., Seifert, R.,  
707 Christof, O.: Methane distribution in European tidal estuaries. *Biogeochemistry* 59, 95–119, 2002.





- 708 Panicker A.S., Pandithurai, G., Beig, G., Kim, D., Lee, D.: Aerosol modulation of ultraviolet radiation  
709 dose over four metro cities in India. *Advances in Meteorology* Article ID 202868, 5 pages, 2014.
- 710 Parsons, T.R., Maita, Y., Lalli, C.M.: A manual of chemical and biological methods for sea water  
711 analysis. New York, Pergamon Press, 1992.
- 712 Purvaja, R., Ramesh R., Frenzel, P.: Plant-mediated methane emission from an Indian mangrove.  
713 *Global Change Biology*, 10, 1–10, 2004.
- 714 Panganiban, A. T., Patt, Jr., T. E., Hanson. R. S.: Oxidation of methane in the absence of oxygen in the  
715 lake water samples. *Appl. Environ. Microbiol.* 37, 303-309, 1979.
- 716 Ray, R., Ganguly, D., Chowdhury, C., Dey, M., Das, S., Dutta, M.K., Mandal, S.K., Majumder, N., De,  
717 T.K., Mukhopadhyay, S.K., Jana, T.K.: Carbon sequestration and annual increase of carbon stock in a  
718 mangrove forest. *Atmospheric Environment*, 45, 5016 – 5024, 2011.
- 719 Reay, W.G., Gallagher, D., Simmons, G.M.: Sediment water column nutrient exchanges in Southern  
720 Chesapeake Bay near shore environments. Virginia Water Resources Research Centre, Bulletin- 181b,  
721 1995.
- 722 Rudolf, K.T., Seigo, S.: Methane and microbes. *Nature* 440, 878 – 879, 2006.
- 723 Rudd, J.W., Taylor, C.W.: Methane cycling in aquatic environments. *Adv. Aquatic Microbial.* 2, 77-  
724 150, 1980.



- 725 Rudd, J. W., M., Hamilton, R.D.: Factors controlling rates of methane oxidation and the distribution of  
726 the methane oxidizers in a small stratified lake. *Arch. Hydrobiol.* 75, 522- 538, 1975.
- 727 Rudd, J. W., M., Hamilton, R.D.: Methane cycling in Lake 227 in perspective with some components of  
728 carbon and oxygen cycles. *Arch. Hydrobiol. Beih. Ergebn. Limnol.* 12, 115-122, 1979.
- 729 Sansone, F.J., Graham, A.W.: Methane along western Mexican margin. *Limnol. Oceanogr.* 49(6), 2242  
730 – 2255, 2004.
- 731 Strangmann, A., Bashan, Y., Giani, L.: Methane in pristine and impaired mangrove soils and its  
732 possible effect on establishment of mangrove seedlings. *Biology and Fertility of Soils*, vol. 44, no. 3,  
733 511-519, 2008.
- 734 Sotomayor, D., Corredor, J.E., Morell, M.J.: Methane flux from mangrove sediments along the  
735 southwestern coast of Puerto Rico. *Estuaries* 17 (1B), 140–147, 1994.
- 736 Smith, S.D., Banke, E.G., 1975. Variation of sea surface drag coefficient with wind speed. *Quarterly*  
737 *Journal of Royal Meteorological Society*, 101, 665–673.
- 738 Utsumi, M., Nojiri, Y., Nakamura, T., Nozawa, T., Otsuki, A., Takamura, N., Watamabe, N., Seki, H.:  
739 Dynamics of dissolved methane and methane oxidation in a dimictic Lake Nojiri during winter. *Limnol.*  
740 *Oceanogr.* 43(1), 10-17, 1998a.



- 741 Utsumi, M., Nojiri, Y., Nakamura, T., Nozawa, T., Otsuki, A., Takamura, N., Watamabe, N., Seki, H.:  
742 Oxidation of dissolved methane in eutropic shallow lake: Lake Kasumigaura, Japan. *Limnol. Oceanogr.*  
743 43(3), 471-480, 1998b
- 744 Upstill-Goddard, R.C., Barnes, J., Frost, T., Punshon, S., Owens, N. J. P.: Methane in the Southern  
745 North Sea: low salinity inputs, estuarine removal and atmospheric flux. *Glob. Biogeochem. Cycles*, 14,  
746 1205–1217, 2000.
- 747 Vaghjiani, G.L., Ravishankara, A.R.: New measurement of the rate coefficient for the reaction of OH  
748 with methane. *Nature* 350, 406 – 409, 1991.
- 749 Wang, Z.P., Delaune, R.D., Patrick Jr., W.H., Masscheleyn, P.H.: Soil redox and pH effects on methane  
750 production in a flooded rice soils. *Soil Sci. Society of America Journal* 57, 382-385, 1993.
- 751 Wayne P.: "Chapter 5: The Earth's Troposphere", *Chemistry of Atmospheres, An Introduction to the*  
752 *Chemistry of Atmospheres of Earth, the Planets and their Satellites*. Oxford Clarendon Press, 209 – 275,  
753 1991.
- 754 Zhang, G., Zhang, J., Lui, S., Ren, J., Xu, J., Zhang, F. : Methane in the Changjiang (Yangtze River)  
755 Estuary and its adjacent marine area: riverine input, sediment release and atmospheric fluxes.  
756 *Biogeochemistry*, 91, 71–84, 2008b.

757



758 **Table 1: Seasonal variation of CH<sub>4</sub> production potential and pore water CH<sub>4</sub> concentrations in**  
 759 **intertidal and sub-tidal sediments. Here, T = soil surface temperature; S = pore water salinity;**  
 760 **[CH<sub>4</sub>]<sub>(PI)</sub> = CH<sub>4</sub> production potential in intertidal sediment; IS = intertidal sediment; SS = sub-**  
 761 **tidal sediment.**

Season	T (°C)	S	Depth (cm)	[CH <sub>4</sub> ] <sub>(PI)</sub> (μmol m <sup>-3</sup> d <sup>-1</sup> )	[CH <sub>4</sub> ] <sub>(IS)</sub> (μM)	[CH <sub>4</sub> ] <sub>(SS)</sub> (μM)
<b>Premonsoon</b>	28.36 ± 1.02	28.88 ± 0.13	0 – 5	ND	2292	2770 ± 1039
			5 – 10	214.99	2313	
			10 – 15	2088.67	2334	
			15 – 20	2918.89	3804	
			20 – 25	4290.22	5274	
<b>Monsoon</b>	28.01 ± 0.41	22.55 ± 0.31	0 – 5	ND	1881	3110 ± 1023
			5 – 10	823.58	2155	
			10 – 15	3539.90	2429	
			15 – 20	4373.44	4508	
			20 – 25	5850.478	6587	
<b>Postmonsoon</b>	18.25 ± 0.22	25.98 ± 0.45	0 – 5	ND	2246	3980 ± 1227
			5 – 10	1175.56	2319	
			10 – 15	4033.30	2413	
			15 – 20	5903.10	4542	
			20 – 25	7352.94	6670	



762 **Table 2: Results of multiple regression analysis between pore water CH<sub>4</sub> concentrations, E<sub>h</sub>, NO<sub>2</sub><sup>-</sup>,**  
763 **SO<sub>4</sub><sup>2-</sup>, AVS and organic carbon (OC) concentration.**

Predictor	Coef	SE Coef	T	P
<b>Constant</b>	10.601	2.921	3.63	0.005
<b>E<sub>h</sub></b>	-0.018447	0.009074	-2.03	0.013
<b>NO<sub>2</sub><sup>-</sup></b>	-0.12277	0.05477	-2.24	0.052
<b>SO<sub>4</sub><sup>2-</sup></b>	- 0.00764	0.01454	-0.53	0.612
<b>AVS</b>	- 0.06933	0.04129	-1.68	0.127
<b>%OC</b>	- 4.086	1.086	-3.76	0.004

764

765

766

767

768



769 **Table 3: Results of multiple regression analysis between surface layer CH<sub>4</sub> oxidation potential**  
770 **([CH<sub>4</sub>]<sub>(ox)</sub>) vs. NH<sub>4</sub><sup>+</sup> & NO<sub>3</sub><sup>-</sup> concentrations .**

Predictor	Coef	SE Coef	T	P
Constant	1.6338	0.3253	5.02	0.015
NH <sub>4</sub> <sup>+</sup>	-0.3065	0.1362	-2.25	0.110
NO <sub>3</sub> <sup>-</sup>	0.2930	0.1285	2.28	0.107

771

772

773

774

775

776

777

778



779 **Table 4: Seasonal variation of dissolved CH<sub>4</sub> concentrations, physicochemical and biological**  
 780 **parameters of estuarine water.**

Properties	Parameters	Position	Premonsoon	Monsoon	Postmonsoon
	[CH <sub>4</sub> ] (nM)	Surface	54.20 ± 5.06	64.58 ± 10.56	90.91 ± 21.20
		Bottom	47.28 ± 12.85	53.27 ± 19.47	67.97 ± 33.12
Physical property	Temperature (°C)	Surface	29.99 ± 0.97	27.82 ± 0.26	19.88 ± 0.18
		Bottom	28.79 ± 0.07	26.92 ± 0.62	19.08 ± 0.78
	S <sub>D</sub> (cm)		62.3 ± 13.1	29.7 ± 7.8	75.9 ± 7.7
Chemical properties	Salinity	Surface	27.09 ± 0.59	19.06 ± 4.33	22.33 ± 0.81
		Bottom	26.88 ± 0.15	18.87 ± 0.33	22.14 ± 0.65
	DO (mg L <sup>-1</sup> )	Surface	6.53 ± 0.29	6.04 ± 0.73	7.27 ± 1.14
		Bottom	5.83 ± 0.37	5.41 ± 0.03	5.98 ± 0.79
	pH	Surface	8.17 ± 0.16	8.10 ± 0.03	8.15 ± 0.06
Biological properties	Chl (µg L <sup>-1</sup> )	Surface	5.30 ± 0.19	3.11 ± 0.39	7.88 ± 1.90
	P (mg C m <sup>-2</sup> hr <sup>-1</sup> )	Surface	56.9 ± 7.1	48.2 ± 8.0	88.0 ± 18.6
	R (mg C m <sup>-2</sup> hr <sup>-1</sup> )	Surface	125.0 ± 100	102.8 ± 116.7	110.1 ± 65.6

781

782

783



784 **Table 5: Results of multiple regression analysis between [CH<sub>4</sub>] and temperature (T) (°C), pH,**  
 785 **chlorophyll (Chl) (µg L<sup>-1</sup>), dissolved oxygen (DO) (mg L<sup>-1</sup>), productivity and community**  
 786 **respiration ratio (P / R).**

Predictor	Coef	SE Coef	T	P
Constant	-296.8	986.5	-0.30	0.792
T	-0.140	2.178	-0.06	0.955
pH	57.6	103.1	0.56	0.633
Chl	2.688	5.801	0.46	0.689
DO	-19.13	28.82	-0.66	0.575
P / R	8.50	61.86	0.14	0.903

787

788

789

790

791





792 **Table 6: Results of multiple regression analysis between dissolved methane consumption rate**  
 793 **( $[\text{CH}_4]_{\text{DOX}}$ ) vs. water temperature (T), salinity (S), dissolved oxygen (DO), DIN, net heterotrophy**  
 794 **(P/R) and secchi disc depth ( $S_d$ ).**

Predictor	Coef	SE Coef	T	P
Constant	-65.85	22.24	-2.96	0.031
T	0.7561	0.6142	1.23	0.273
S	2.1752	0.4949	4.40	0.007
DO	7.528	2.868	2.62	0.047
DIN	-0.4082	0.3686	-1.11	0.318
P/R	-2.012	2.938	-0.68	0.524
$S_d$	-0.30365	0.09738	-3.12	0.026

795

796

797

798

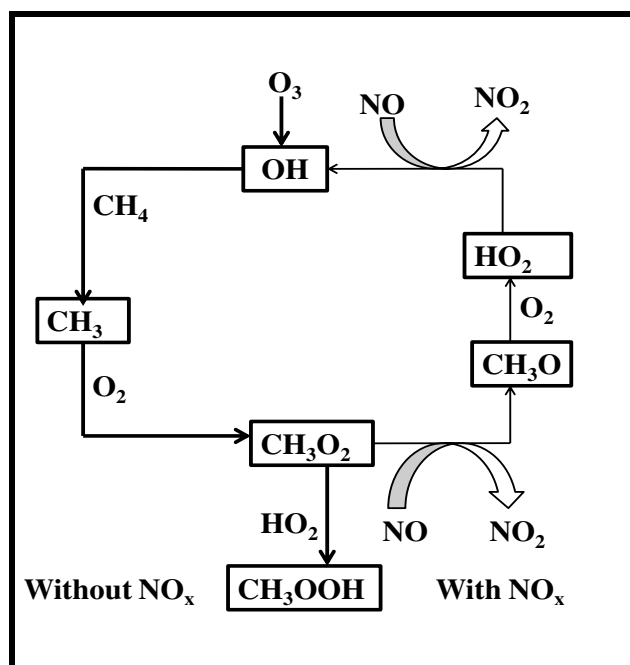


799 **Table 7: Seasonal variation of micrometeorological parameters, methane mixing ratio, biosphere**  
 800 **– atmosphere CH<sub>4</sub> exchange and CH<sub>4</sub> photo-oxidation in mangrove forest atmosphere.**

Parameters	Height(m)	Premonsoon	Monsoon	Postmonsoon
Air temp. (°C)	10	30.34 ± 0.91	29.74 ± 2.50	17.34 ± 4.09
	20	29.73 ± 1.13	28.37 ± 0.88	16.17 ± 1.80
Wind velocity(ms <sup>-1</sup> )	10	0.70 ± 0.42	1.32 ± 1.11	0.41 ± 0.36
	20	0.95 ± 0.44	1.64 ± 1.37	0.80 ± 0.88
U* (m/sec)		0.20 ± 0.04	0.15 ± 0.15	0.17 ± 0.49
Z <sub>o</sub> (m)		3.77 ± 3.01	1.63 ± 1.02	2.97 ± 2.98
C <sub>D(10m)</sub>		0.386	0.157	0.167
H (W m <sup>-2</sup> )		6.349	8.248	1.154
PBL (m)		936.59	702.45	796.10
CH <sub>4</sub> (ppmv)	10	1.769 ± 0.04	2.180 ± 0.12	2.112 ± 0.05
	20	1.821 ± 0.09	2.027 ± 0.03	2.116 ± 0.06
F <sub>BA</sub> (mg m <sup>-2</sup> hr <sup>-1</sup> )		- 4.514	6.635	-2.110
[CH <sub>4</sub> ] <sub>photo-ox rate</sub> (molecules cm <sup>-3</sup> d <sup>-1</sup> )	10	1.40 x 10 <sup>11</sup>	1.67 x 10 <sup>11</sup>	6.05 x 10 <sup>10</sup>

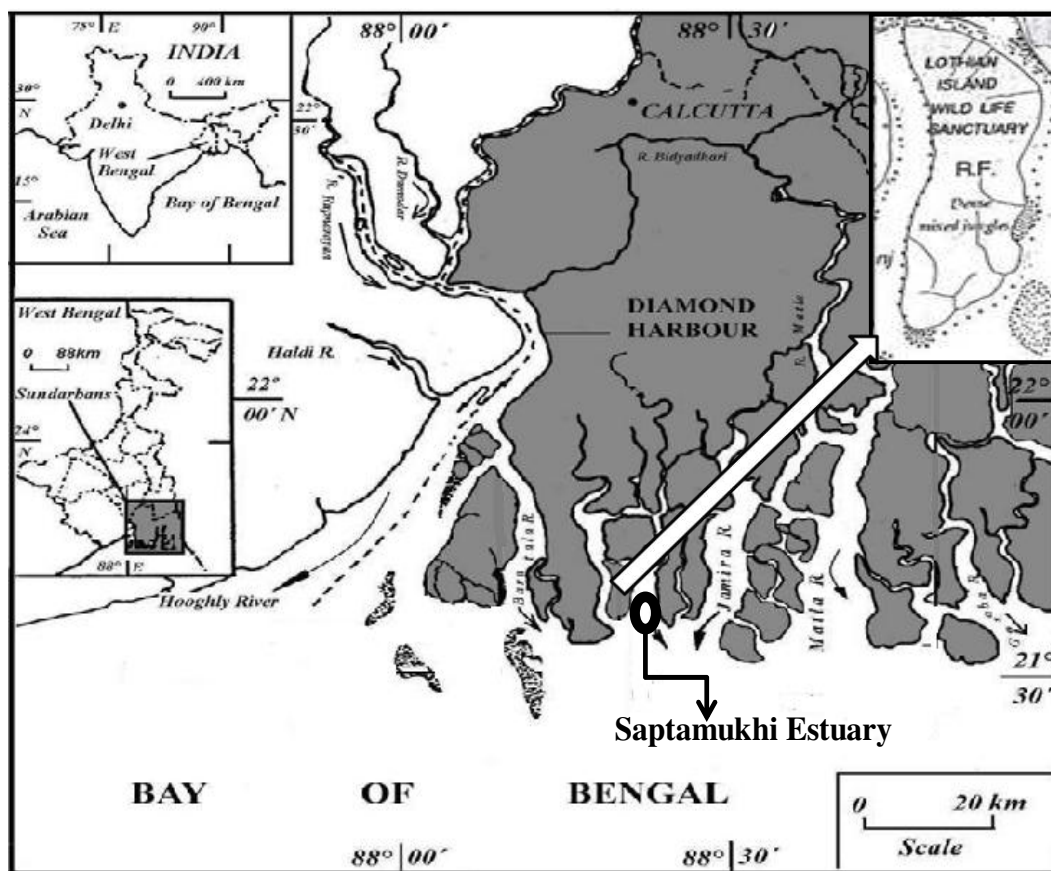


801



802

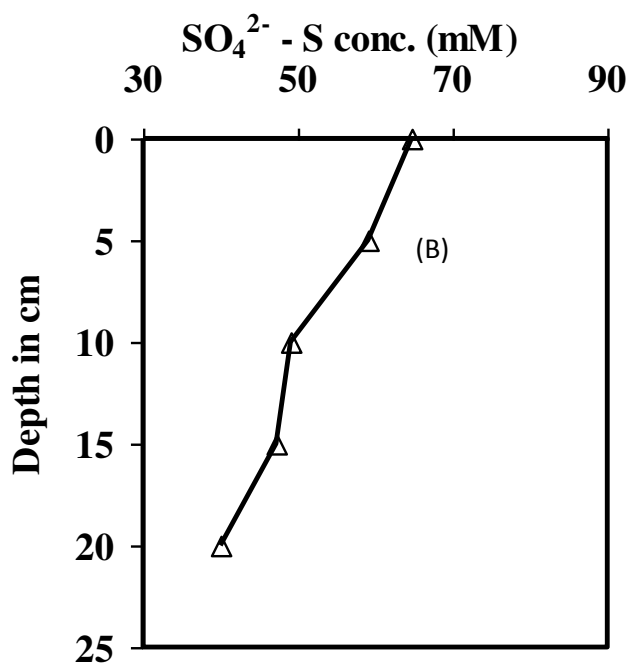
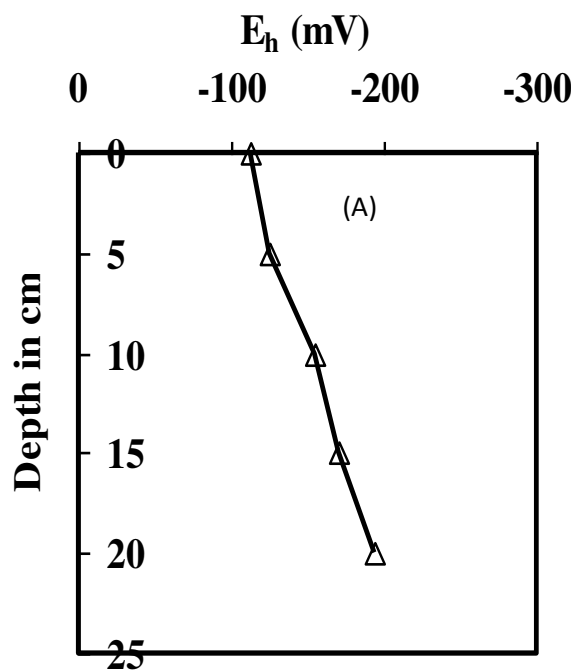
803 Fig.1: Schematic diagram of atmospheric CH<sub>4</sub> photooxidation with/without NO<sub>x</sub> concentration.



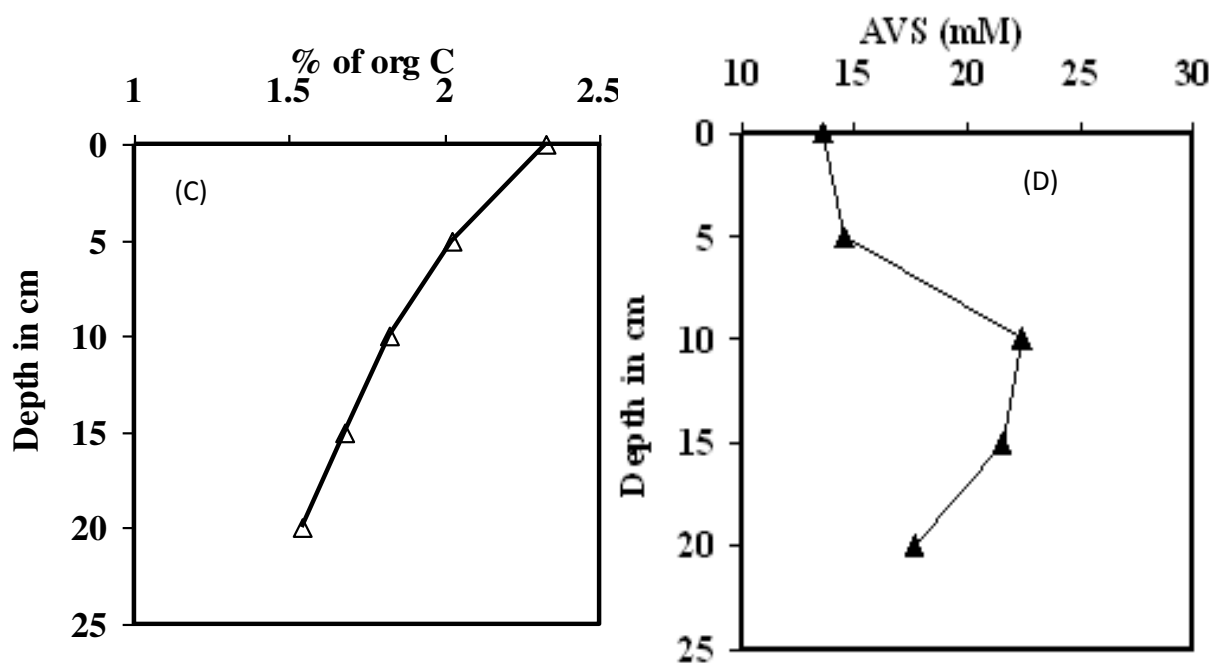
804

805

Fig.2: Map showing locations of the study point.

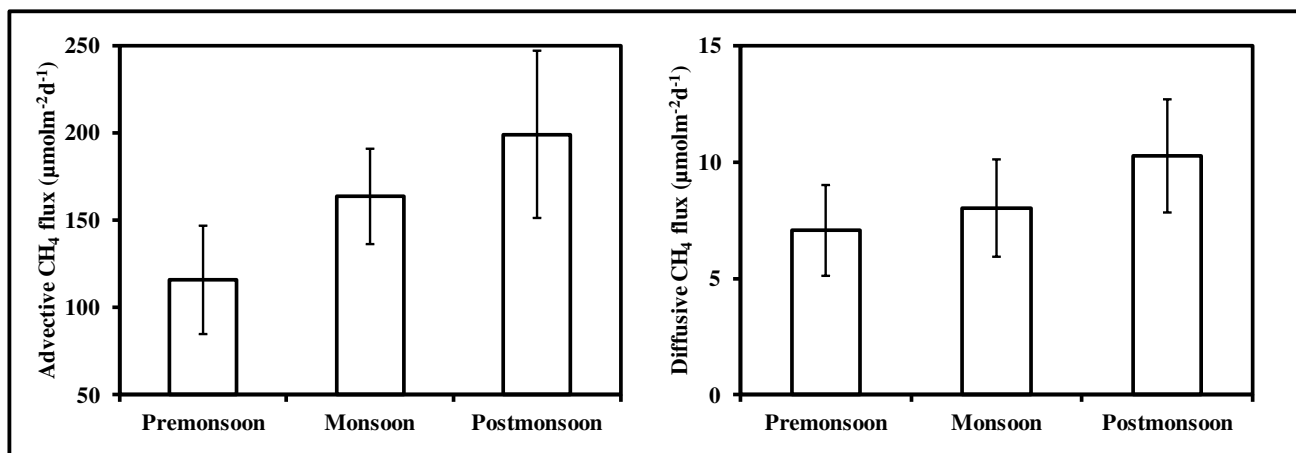


806

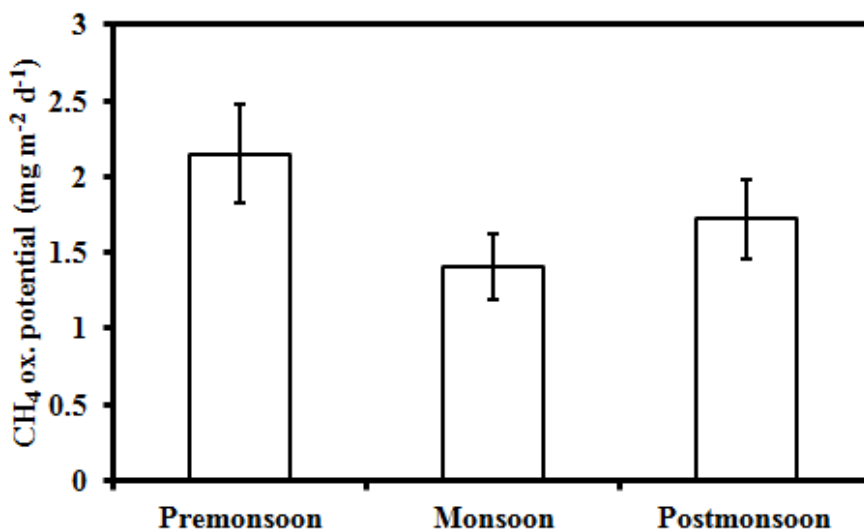


807

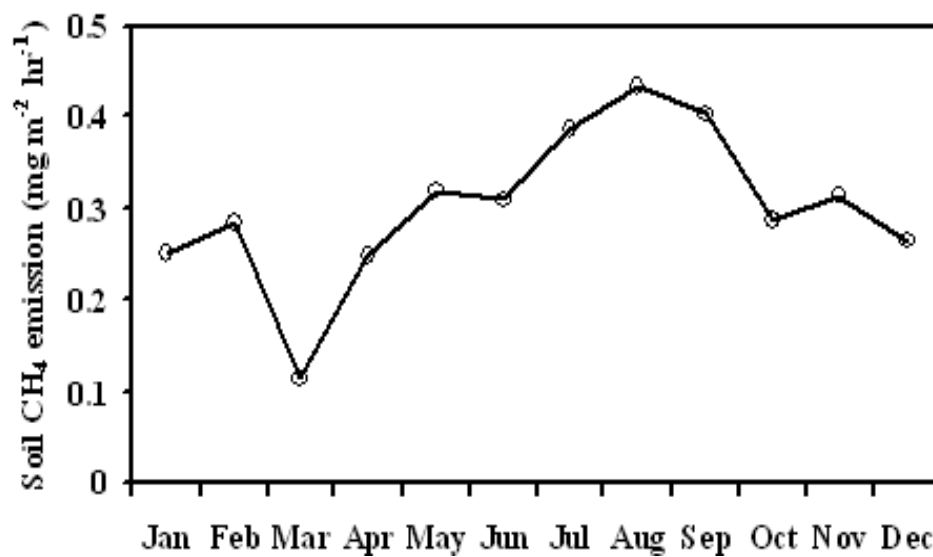
808 Fig.3: Vertical variation of physicochemical properties of mangrove sediment (A)  $E_h$  (B) pore water  
809 sulphate – S concentration (C) % organic carbon (D) pore water AVS concentration



810  
811 Fig.4: Seasonal variation of advective and diffusive CH<sub>4</sub> fluxes from intertidal and subtidal sediments,  
812 respectively.

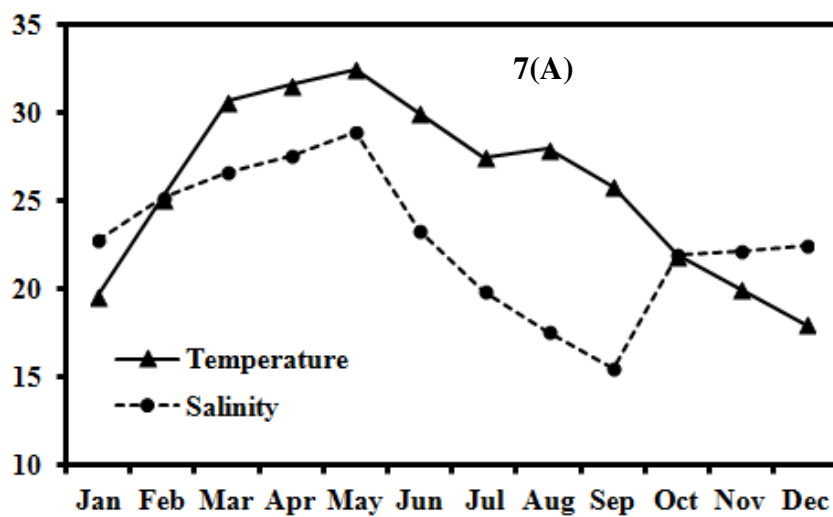


813  
814 Fig.5: Seasonal variations of surface sediment CH<sub>4</sub> oxidation potential in mangrove sediment.



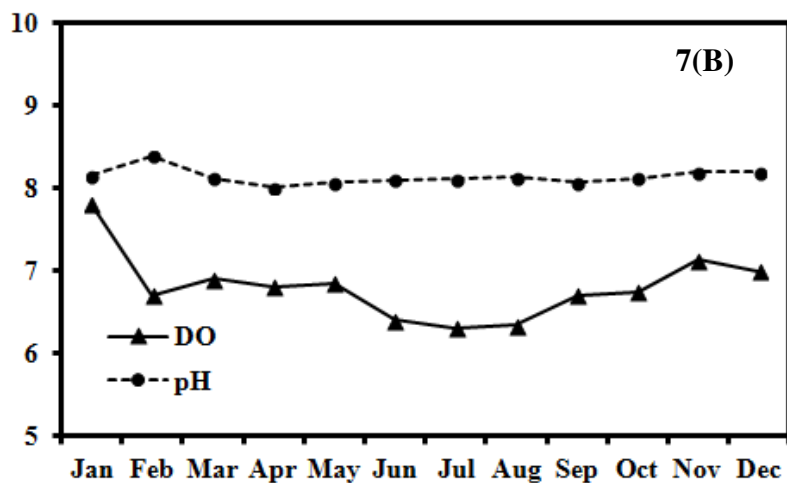
815

816 Fig.6: Monthly variation of soil methane emission from intertidal mangrove forest.

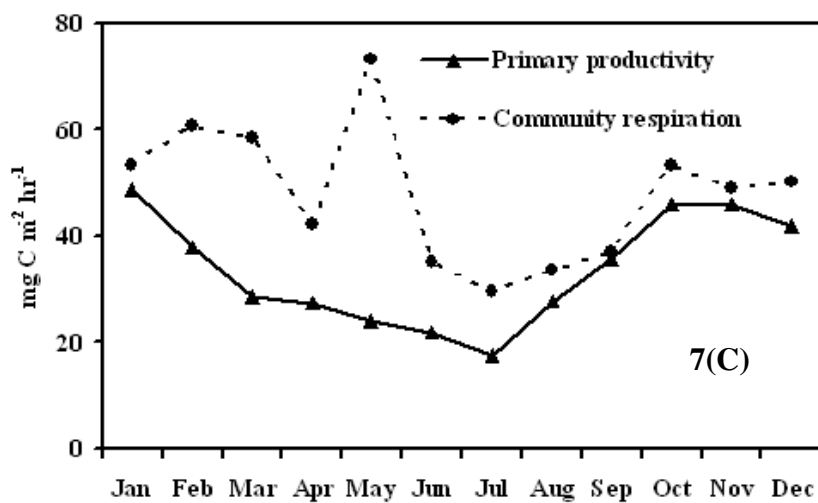


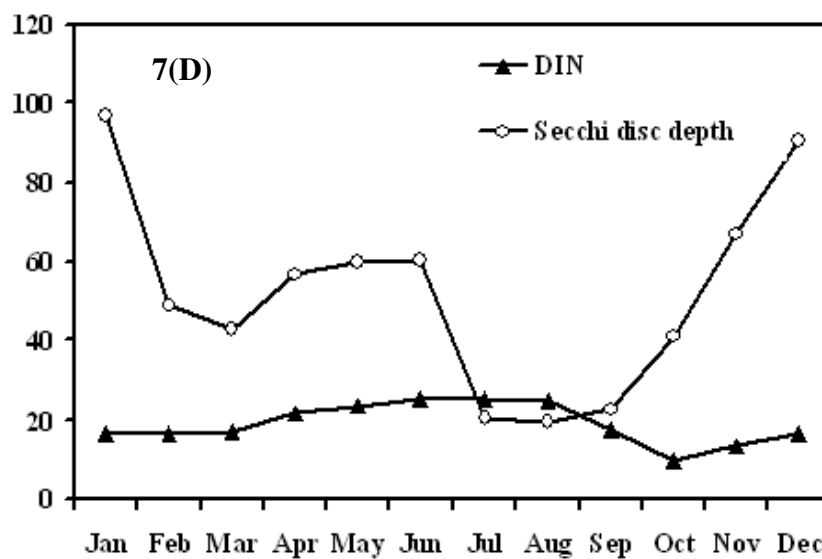
817



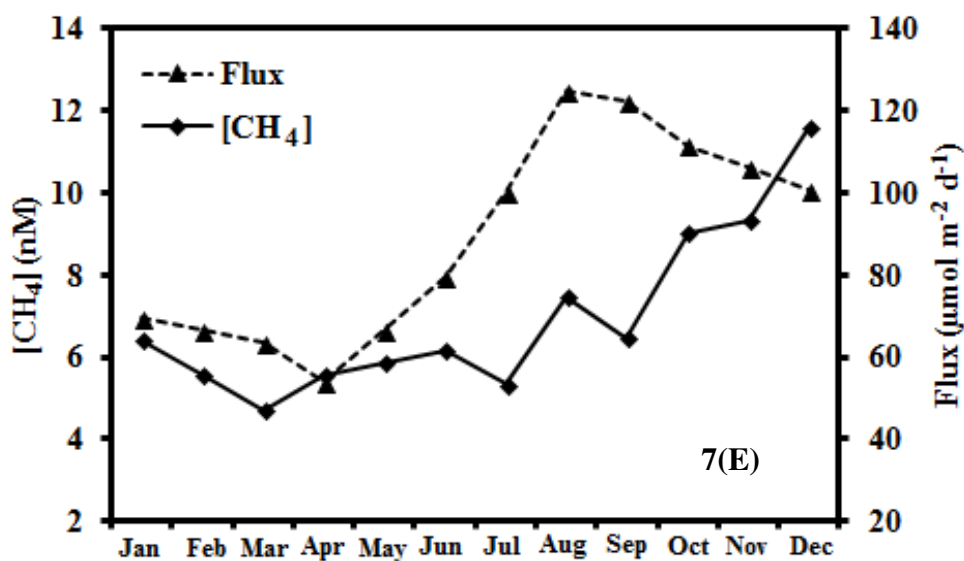


818



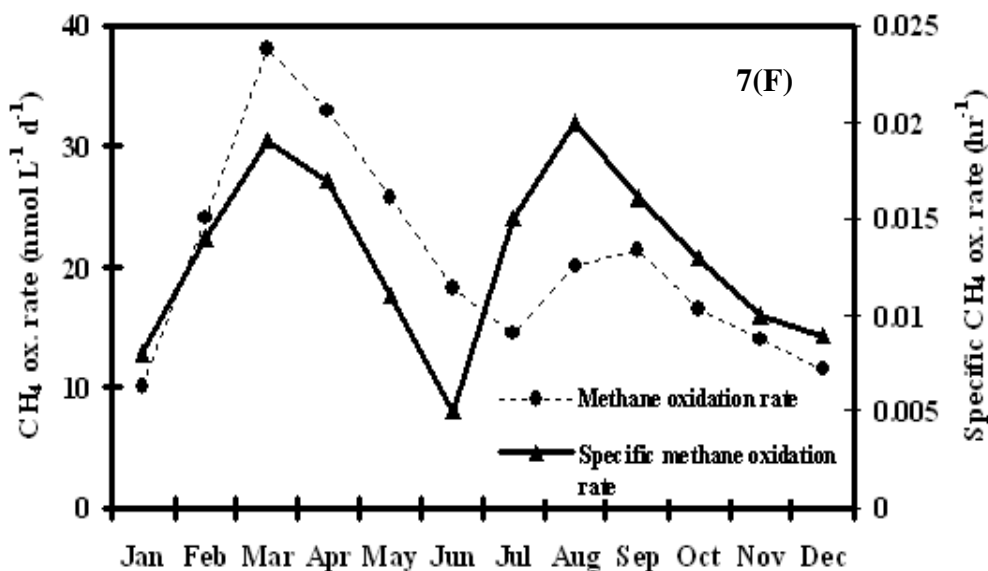


824



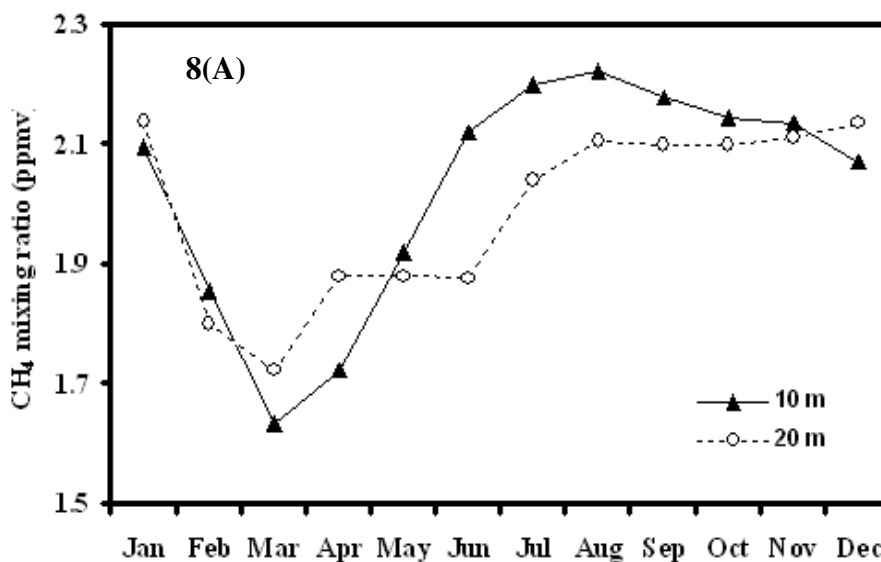
825

826

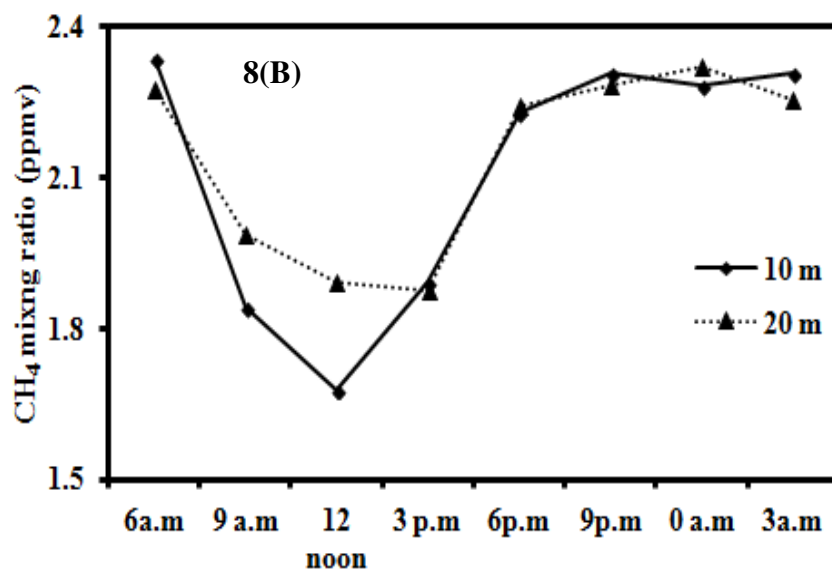


827

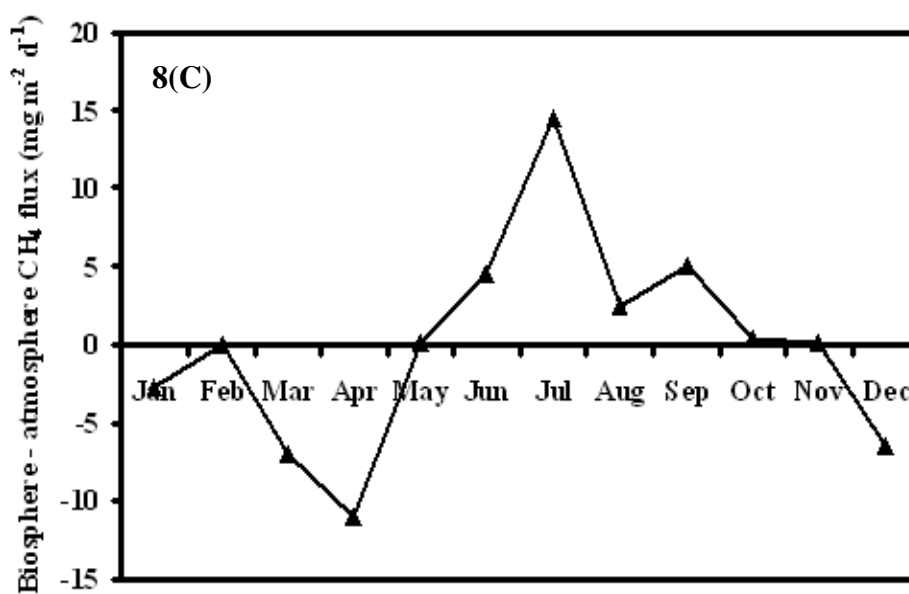
828 Fig.7: Monthly variation of physicochemical parameters along with dissolved methane concentrations,  
 829 methane oxidation and air-water methane exchange flux.



830



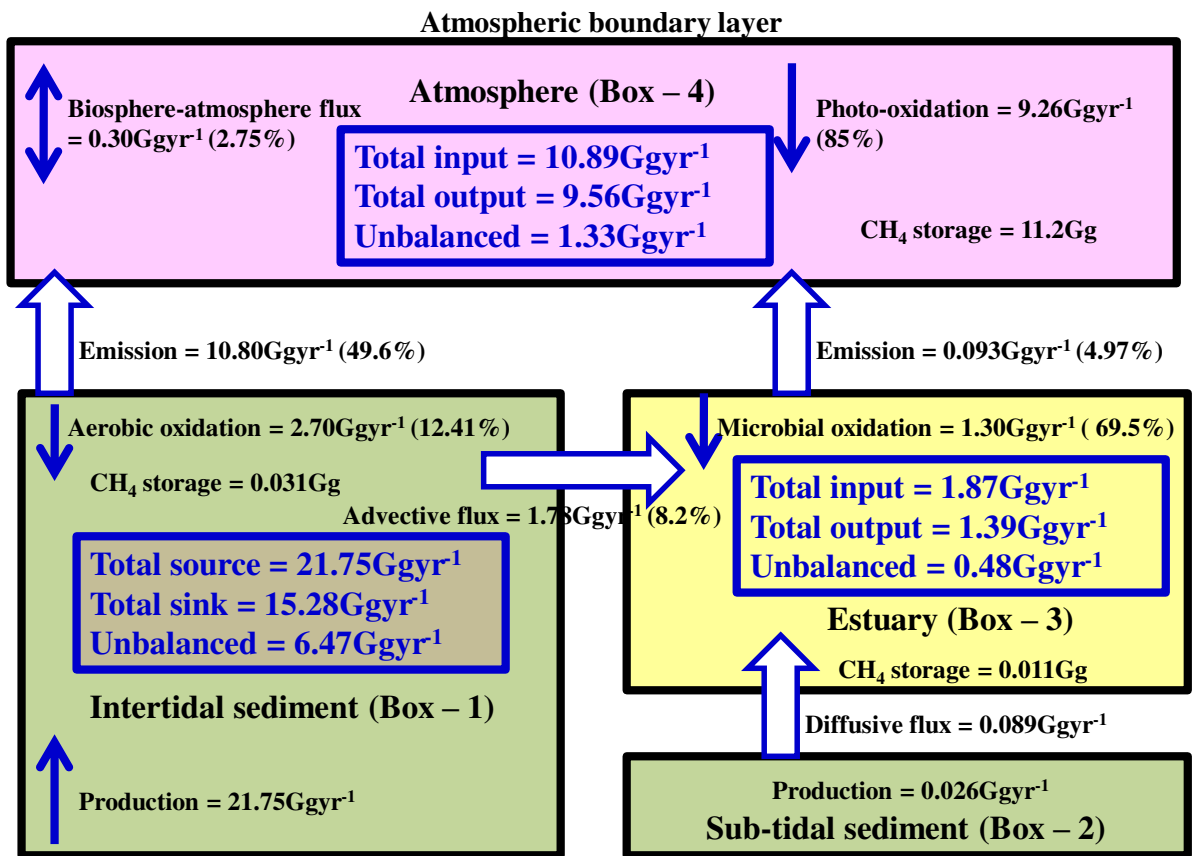
831



832



833 Fig.8: (A) Monthly variation of methane mixing ratio in forest atmosphere (B) Diurnal variation of  
 834 methane mixing ratio in forest atmosphere (C) Monthly variation of biosphere-atmosphere methane  
 835 exchange flux.



836

837 Fig.9: Quantitative methane budget at Sundarbans mangrove ecosystem.

838